Smaller Satellites, Bigger Return

Microsatellite Development, Testing and On-Orbit Operation

Departmental MASc Seminar

Emerson Vargas Niño

Supervisor: Dr. Robert E. Zee

September 22, 2022

Motivation

- The miniaturization and availability of low-cost spacecraft components in the past few decades have led to the emergence of smaller, less expensive spacecraft, which do not need to be large to be useful.
- This, combined with the rise of lower-cost launch opportunities, such as ride-share missions, has led to the democratization of space
- This, in turn, has led to a substantial increase in the number of spacecraft launched, particularly small spacecraft.
- In recent years, over 90% of all satellites launched have been small spacecraft, with an overall mass under 600 kg
- This motivates the study and development of small satellite platforms

The DEFIANT Platform

- A recent spacecraft platform developed at SFL is DEFIANT
- It features a large payload bay volume and deployable wings
- The design, analysis and on-orbit operation of DEFIANT-class spacecraft is the subject of this thesis

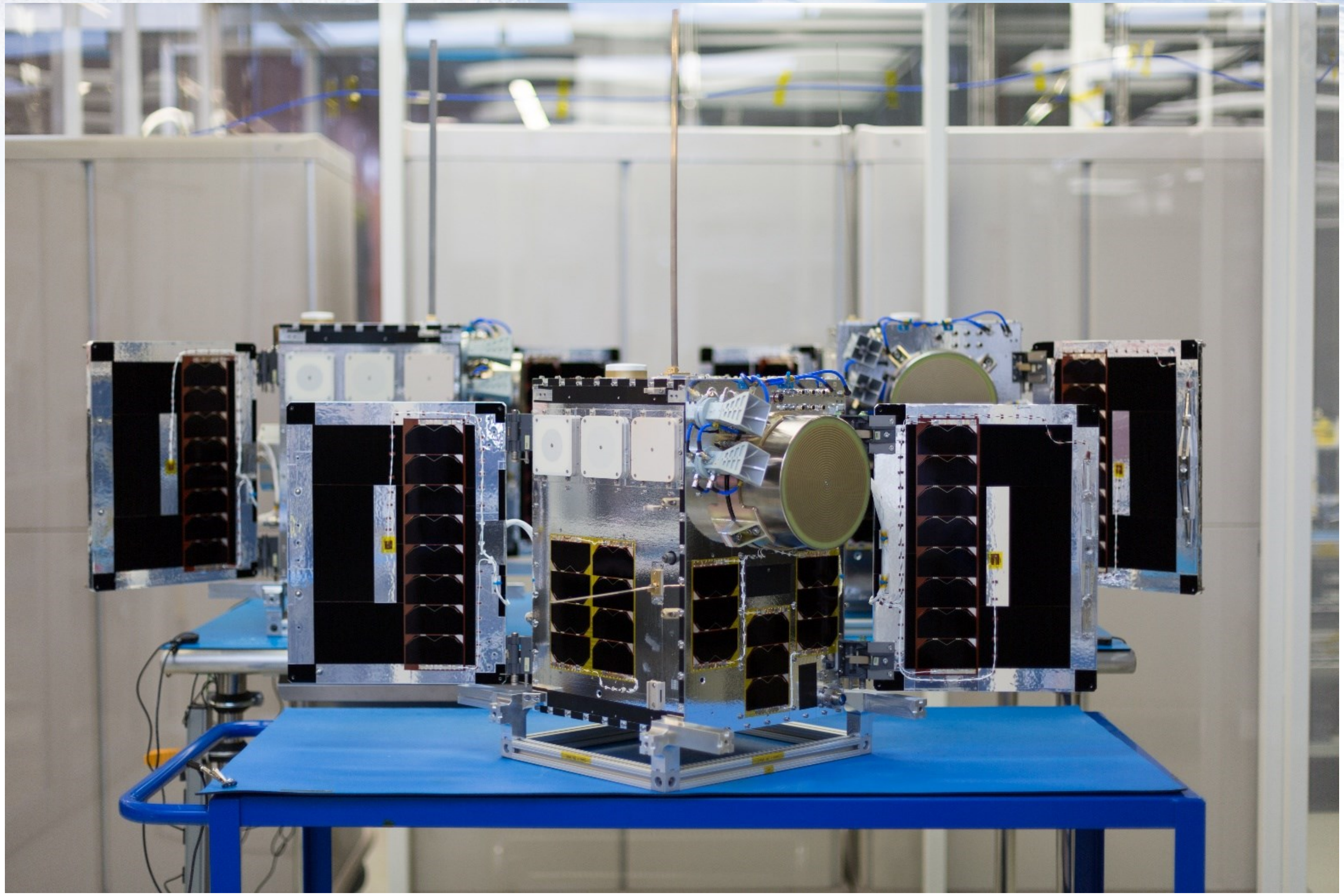

Thesis Overview

- Microsatellite spacecraft use has increased substantially in recent years, motivating the investigation into their design, testing and on-orbit operations, as the combination of these aspects is critical to the success of a microsatellite mission
- The work presented is centered around SFL's DEFIANT platform, but given the generic nature of SFL spacecraft platforms, it has the opportunity to be applied to future SFL platforms, as well
- This thesis details the development of multiple spacecraft subsystems for this platform, including the GNC, propulsion and deployable solar panel
- The work outlined was used in the design, analysis, testing and commissioning of over 20 spacecraft for SFL, supporting its competitive advantage in the microsatellite world market

Guidance, Navigation and Control System

- The GNC system is responsible for three main operations:
  - **Guidance**: determination of desired attitude and orbital state
  - **Navigation**: determination of attitude and orbital state
  - **Control**: determination of actuation necessary to achieve desired state
- Broadly separated into:
  - GNC Hardware
  - GNC Software

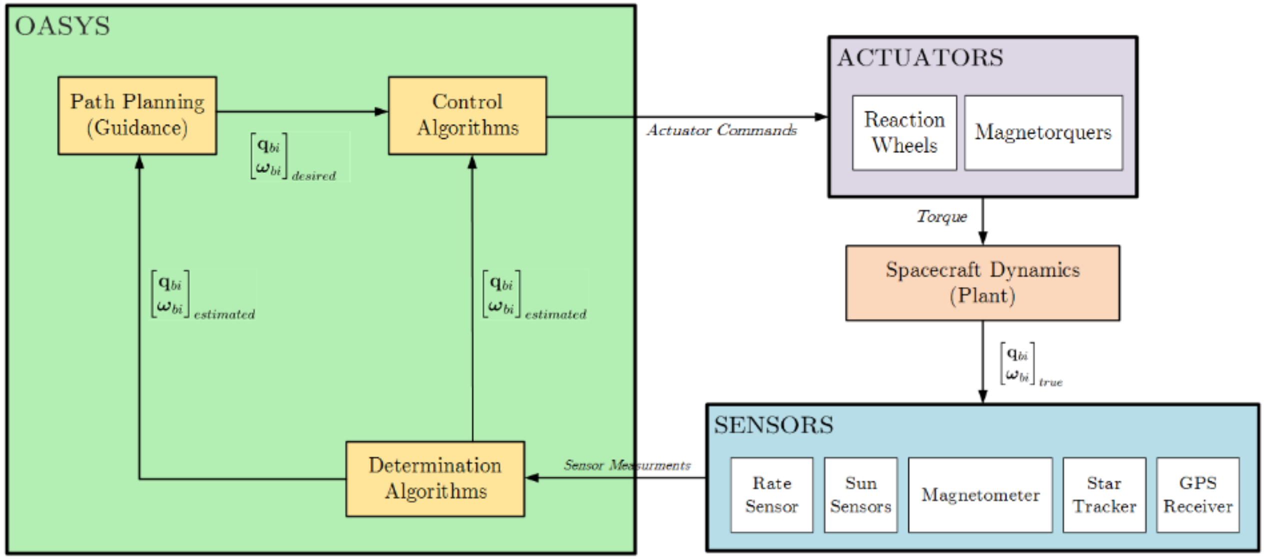

GNC Hardware

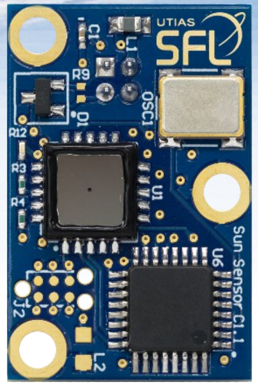

Sun Sensor

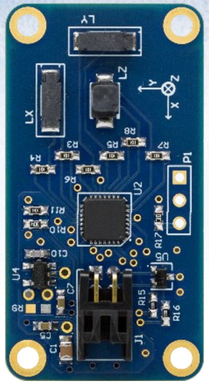

Magnetometer

Rate Sensor

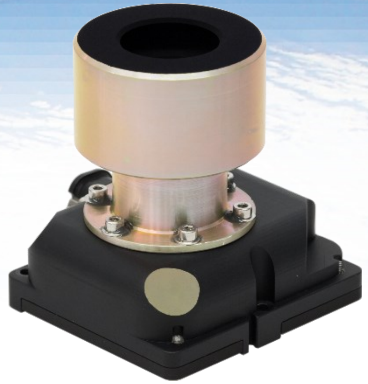

Star Tracker

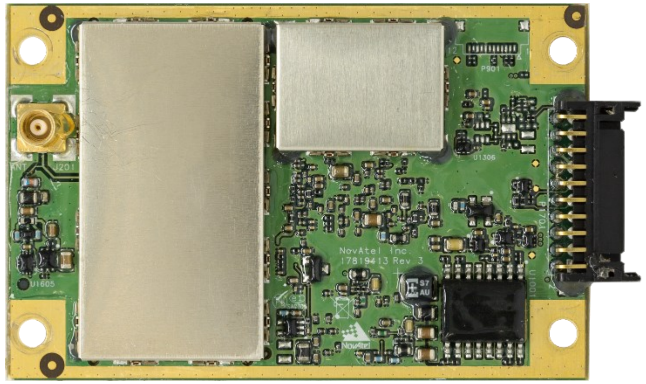

GPS Receiver

GPS Antenna

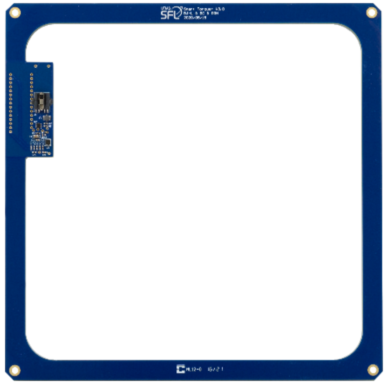

Magnetorquer

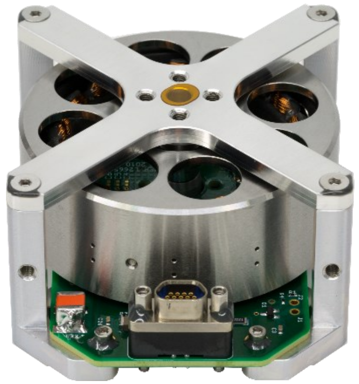

Reaction Wheel

GNC Hardware

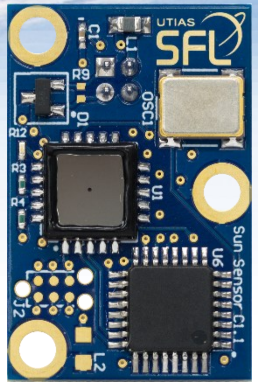

Sun Sensor

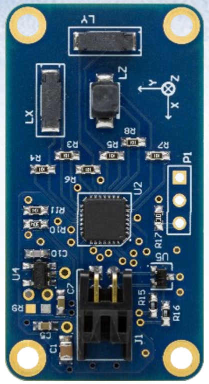

Magnetometer

Rate Sensor

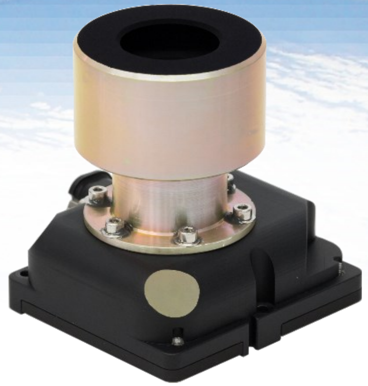

Star Tracker

Coarse Attitude Determination

Fine Attitude Determination

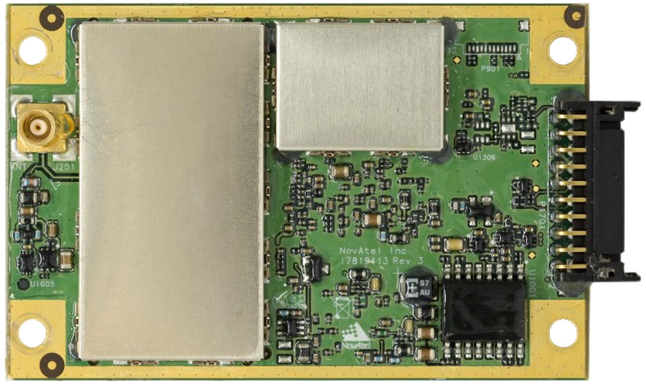

GPS Receiver

GPS Antenna

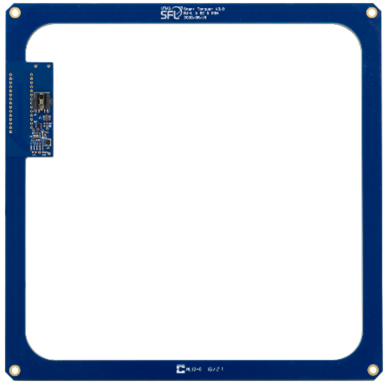

Magnetorquer

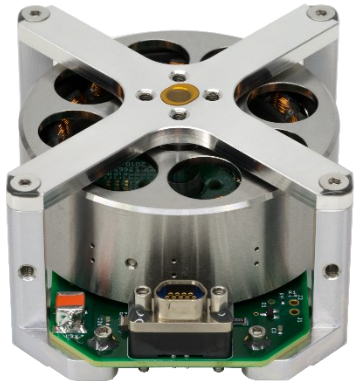

Reaction Wheel

GNC Hardware

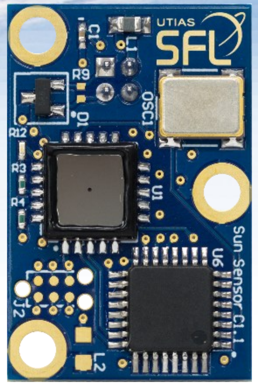

Sun Sensor

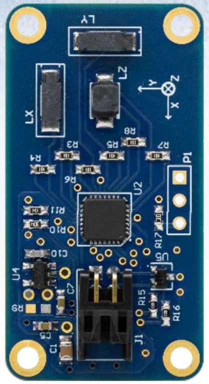
Magnetometer


Rate Sensor

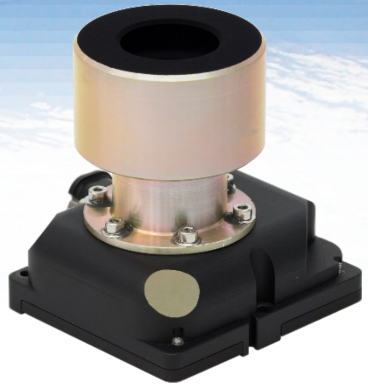
Star Tracker

Orbit Determination

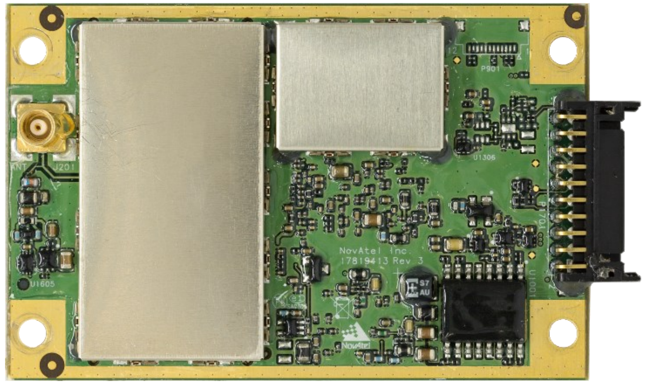
GPS Receiver


GPS Antenna

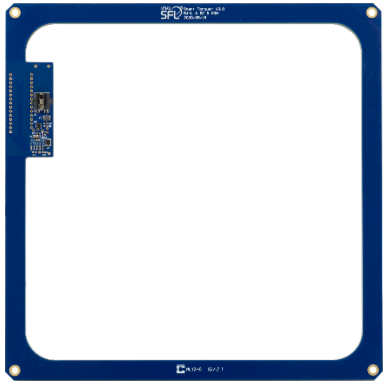
Magnetorquer

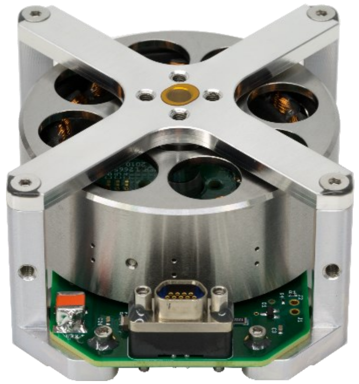
Reaction Wheel

GNC Hardware

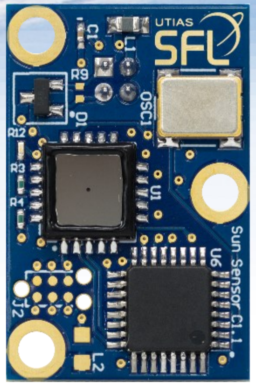
Sun Sensor

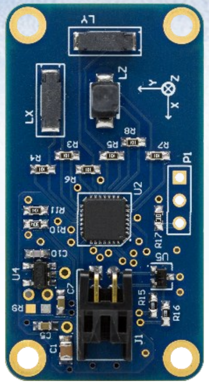
Magnetometer


Rate Sensor

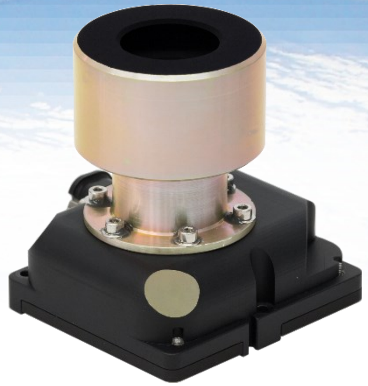
Star Tracker

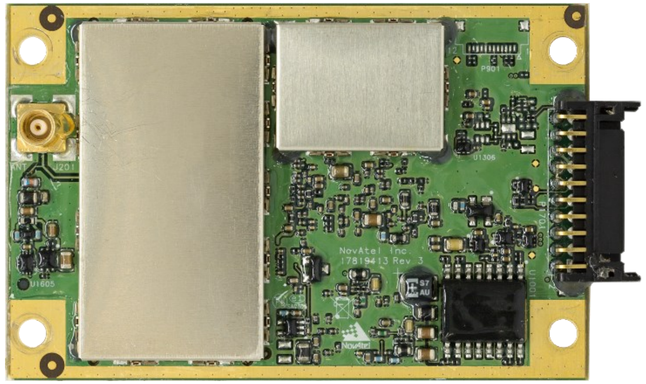
GPS Receiver


GPS Antenna

Attitude Actuators

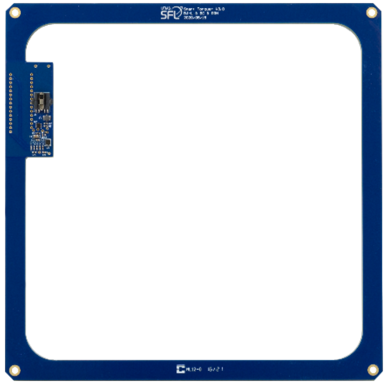
Magnetorquer

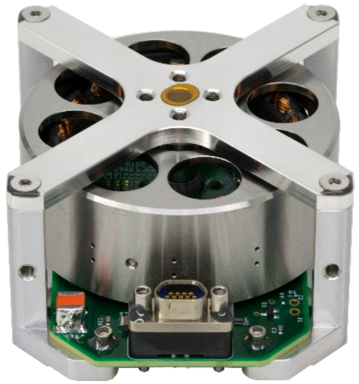
Reaction Wheel

UTIAS SFL

GNC Hardware

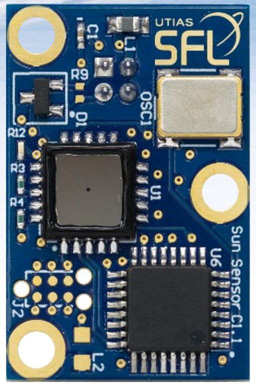
Sun Sensor

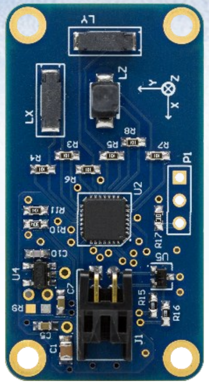
Magnetometer


Rate Sensor

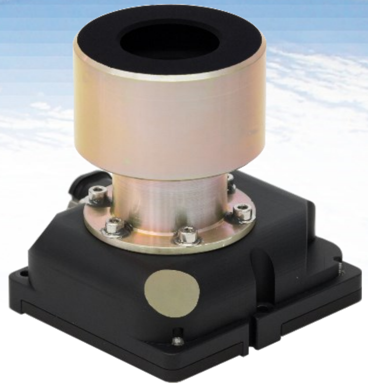
Star Tracker

Calibrated In-house

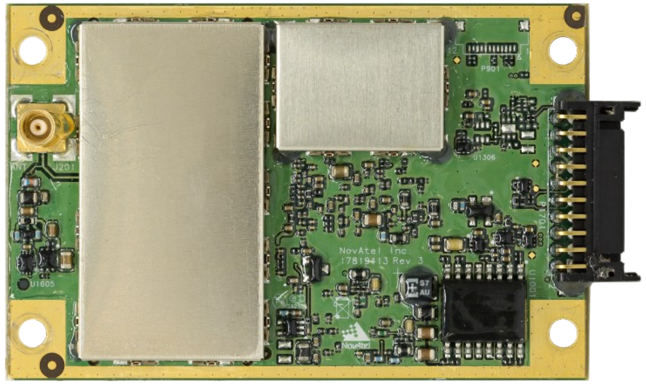
GPS Receiver


GPS Antenna

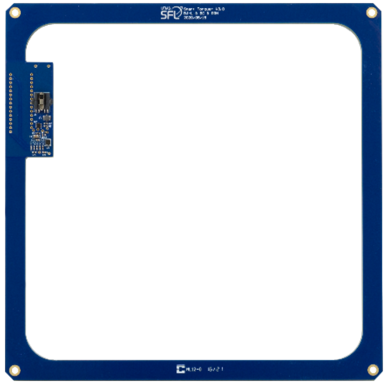
Magnetorquer

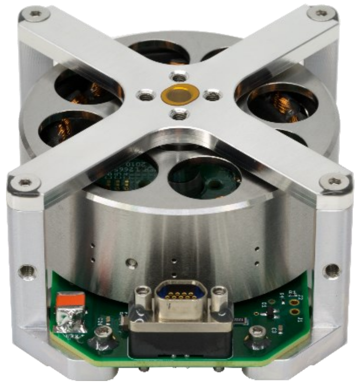
Reaction Wheel

Sensor Calibration

- Manufacturing tolerances lead to many sensors using an error model that relate the raw sensor output to a corrected measurement vector
- Error model parameters determined through a sensor calibration
- All sensor calibrations follows the same outline:
  - **Data collection:** sensor is placed in a test apparatus able to vary the parameter that the sensor measures. Truth data is collected from apparatus, measurement data from the sensor
  - **Optimization**: Error model parameters found by solving an optimization problem that finds parameters which minimize residual between truth and measured data

$$\boldsymbol{\omega} = \left(\mathbf{1} + \mathbf{S} + \mathbf{C}_{\mathrm{N}}\right)^{-1}\left(\breve{\boldsymbol{\omega}} - \mathbf{O}\right)$$

$$\underset{\mathbf{x}}{\text{minimize}} \quad \left| \left|\boldsymbol{\omega}_{\mathrm{r},k}\right|^2 - \left|\boldsymbol{\omega}_k\left(\mathbf{x}\right)\right|^2 \right|^2$$

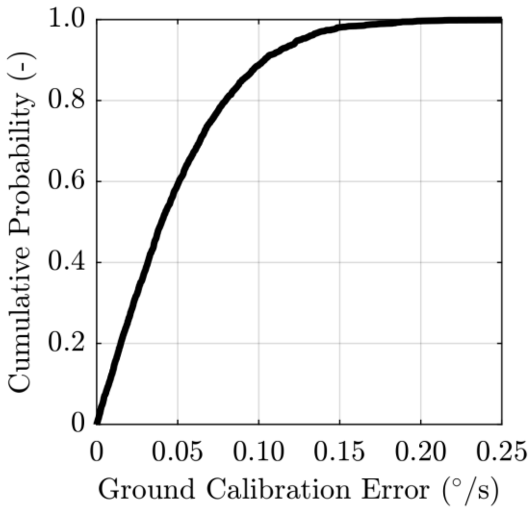

Star Tracker

- Tracks the position of stars to generate attitude solutions
- Most accurate solutions out of all determination sensors but with rate & illumination constraints
- Small and Large Baffle options
- Maximum slew rate
  - 3°/second
- Small Baffle STR avoidance angles
  - 45° sun-to-boresight
  - 22° Earth's limb-to-boresight

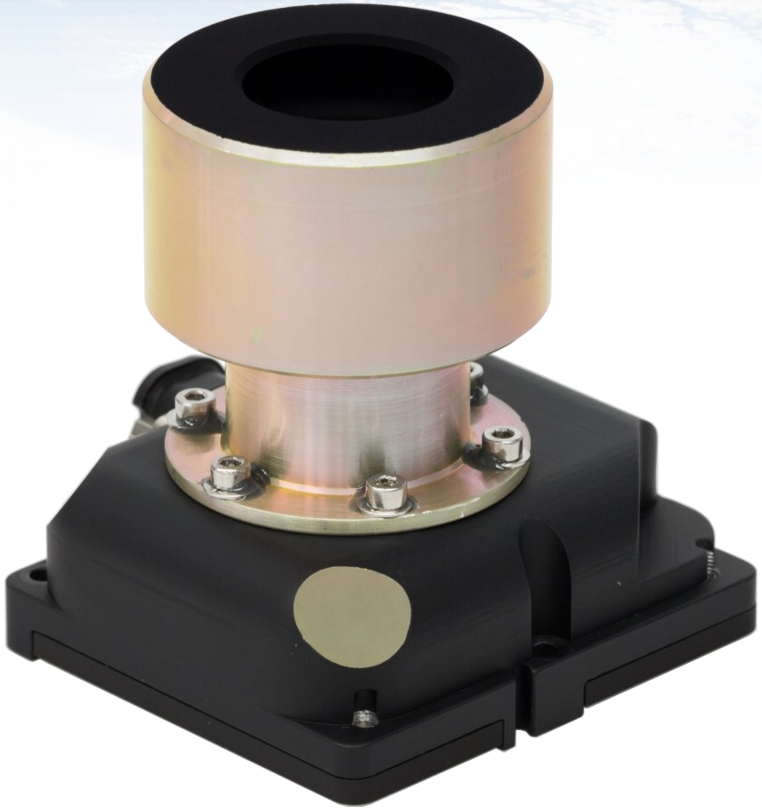

GNC Software: Guidance

- Align-constrain guidance algorithm calculating desired attitude, angular velocity and angular acceleration with two objectives:
  - **Primary:** align a spacecraft body vector to a target
  - **Secondary:** constrain separate spacecraft body vector as close as possible to separate target

Body vector to align	Payload boresight
Inertial vector to align to	Satellite to ground station
Body vector to constrain	STR boresight
Inertial vector to constrain to	***Weighted Sum Constraint Vector***

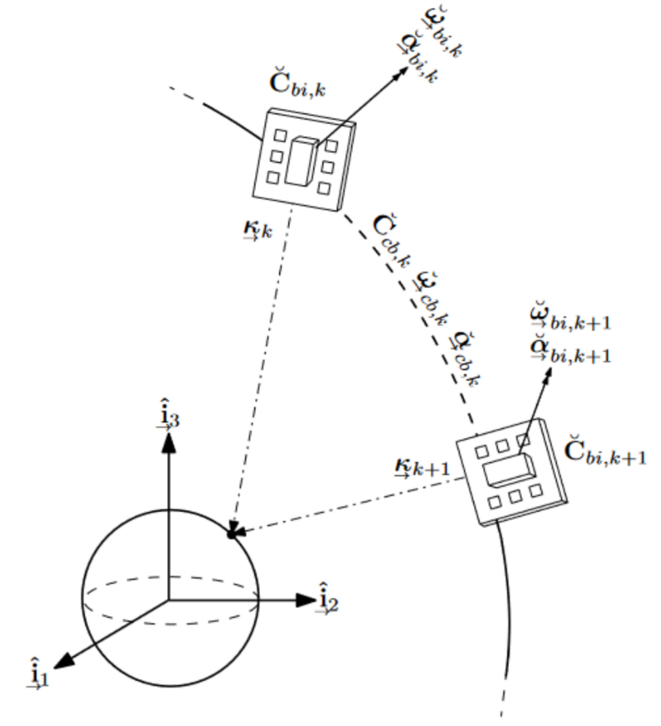

UTIAS

Weighted Sum Constraint Vector

- Derived by need to point away from the Sun and Earth's limb
- Minimizes star tracker illumination constraint violations by maximizing distance between star tracker boresight vector and:
  - nadir unit vector
  - Sun unit vector
- Linear combination of anti-nadir unit vector $\boldsymbol{n}'$ and anti-Sun unit vector $\boldsymbol{s}'$
  - Scaled by constants c_n and c_s respectively, where $c_n = [0, 1]$ and $c_s = 1 - c_n$

$$\mathbf{w} = c_{\mathrm{n}}\mathbf{n}' + c_{\mathrm{s}}\mathbf{s}'$$

Flight Software & Flight Simulation

- OASYS
  - Main attitude software onboard all SFL spacecraft
  - Implements GNC algorithms
  - Unifies hardware and software GNC systems
- MIRAGE
  - Simulation environment written in MATLAB and Simulink
  - Interfaces with OASYS and has representative models for all GNC hardware
  - Used to predict and validate GNC system's on-orbit performance against mission requirements

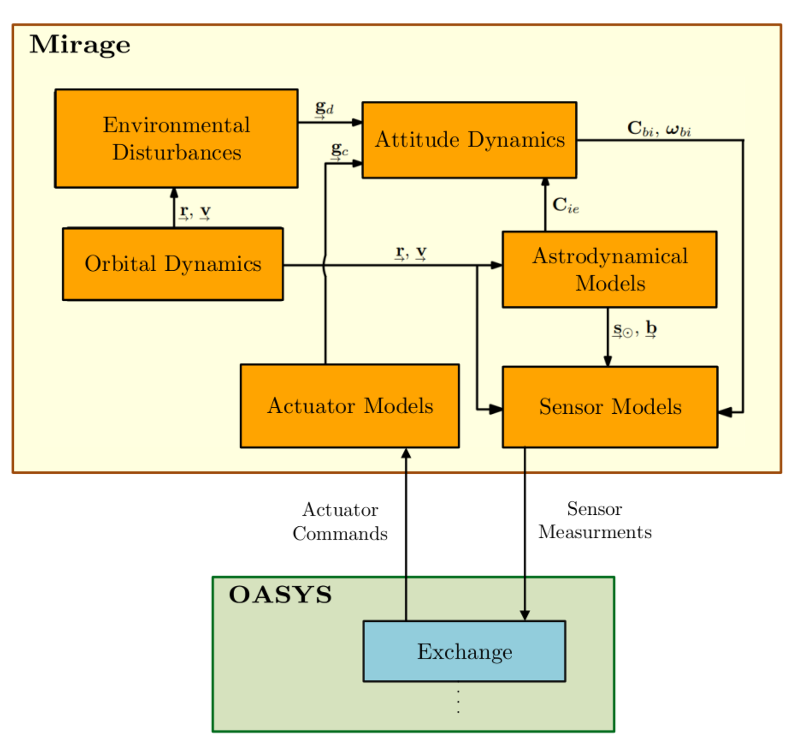

ROSA: **R**apid **O**ptimization of **S**pacecraft **A**ttitudes

- New simulation environment written in Python for rapid evaluation and optimization of spacecraft attitude trajectories, sensor placements and wheel momentum setpoints
  - Interfaces with STK to automate scenario creation
  - Implements modified guidance algorithm using numerical differentiation, instead of analytical solution, for angular velocity and acceleration solution
  - Implements stochastic and gradient-based optimization methods
- ROSA has a reduced scope but is significantly faster than MIRAGE
  - Only executes algorithms as necessary
  - Uses a variety of techniques to speed up its execution
    - C or FORTRAN subroutines called within Python for numerical methods
    - Just-in-time (JIT) compilation and parallelization provide further speed ups

Star Tracker Implementation

- Star tracker implementation into the DEFIANT bus is separated into 2 stages
- **1st Stage:** determination of star tracker placement
  - Early in mission timeline, as spacecraft structure manufacturing has long lead times
  - Orbit not finalized as launch contract has not been signed yet
  - Placement that is effective across all possible orbits must be selected
- **2nd Stage:** determination of trajectory to maximize star tracker effectiveness
  - Late in mission timeline
  - Orbit finalized as launch contract has been signed
  - Star tracker orientation cannot be altered anymore, but spacecraft trajectory can still be adjusted to maximize star tracker effectiveness

UTIAS SFL

Star Tracker Orientation Parametrization

- Payload and star tracker orientation parameterized through azimuth-elevation: $(\theta, \phi)°$
- Payload is assumed to be at $(0, 90)°$
- Star tracker boresight ranges as follows:
  - Azimuth: 0°
  - Elevation: [-90°, 90°]
- Results are symmetrical about azimuth as payload rotates freely about its boresight

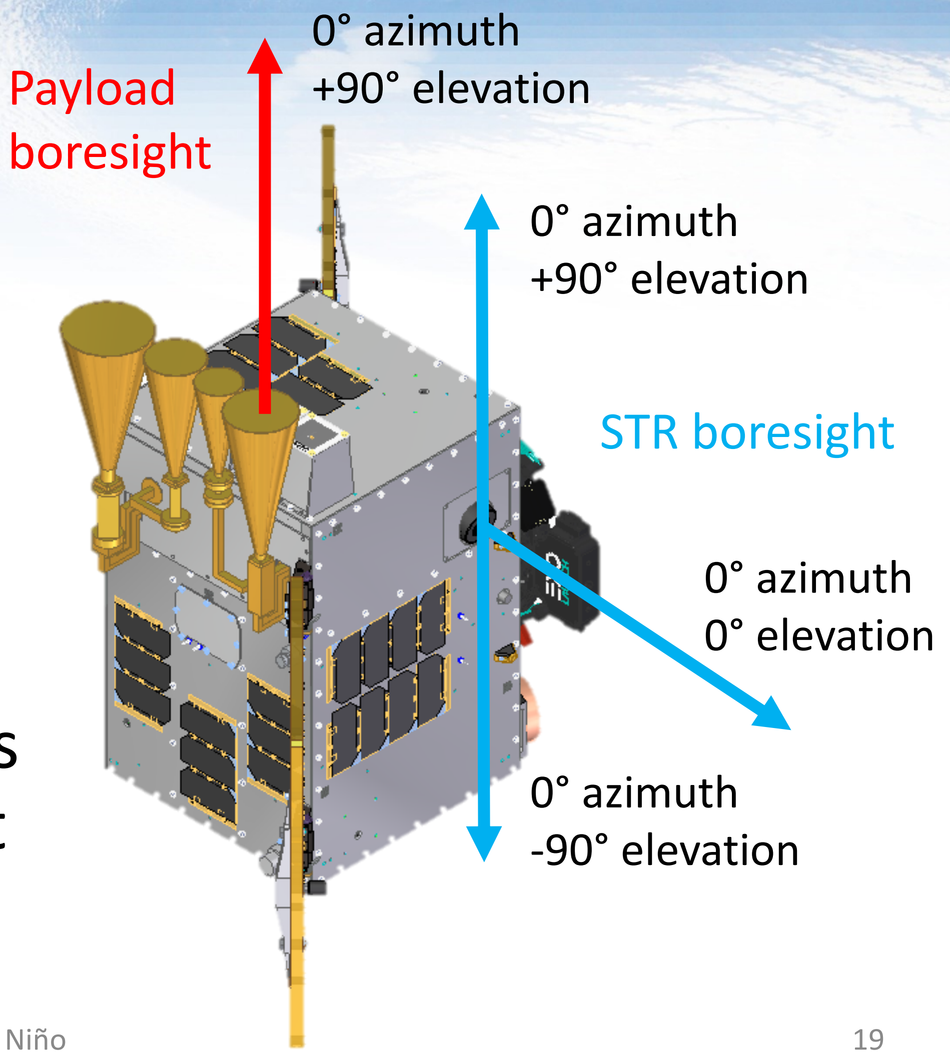

Star Tracker Effectiveness

- A Star tracker is:
  - **Available:** if illumination & rate constraints aren't violated
  - **Effective:** if available & if trajectory is kinematically feasible, such that it doesn't violate actuation capabilities of reaction wheels
- A pass is effective if composed of >80% continuous, effective timesteps
- ROSA is used to calculate $\mathcal{E}$, a numerical effectiveness function
  - **Input:** Orbit, operational scenario, star tracker orientation, trajectory
  - **Output:** Mean effectiveness of scenario passes

Numerical Optimization

- **1st Stage:** determination of star tracker placement, given by star tracker elevation ϕ, that is effective across all orbits being considered

$$\underset{\phi,\, c_\mathrm{n}}{\text{minimize}} \qquad -\frac{1}{m}\sum_{i=1}^{m} \mathcal{E}_i(\phi, c_\mathrm{n})$$

- **2nd Stage:** determination of trajectory to maximize star tracker effectiveness, given a chosen orbit and a fixed star tracker elevation ϕ

$$\underset{c_\mathrm{n}}{\text{minimize}} \qquad -\mathcal{E}(\phi, c_\mathrm{n})$$

UTIAS SFL

Operational Scenarios

	Mission 1	Mission 2
Orbits	Four SSO at 1000 km altitude	Five circular orbits at 550 km altitude
LTAN	10:00, 11:00, 15:05, and 21:00	42° inclination and four SSO with LTANs of 6:00, 9:30, 11:00, and 13:30
Payload Pointing Target	Ground station near Toronto	SSO orbits: Hawaii, Svalbard, Troll ground stations 42° orbit: Hawaii ground station
Baffles	Small only	Small and Large
Limits	Star tracker elevation limited to [-15, 15]	No limits to star tracker elevation

Mission 1

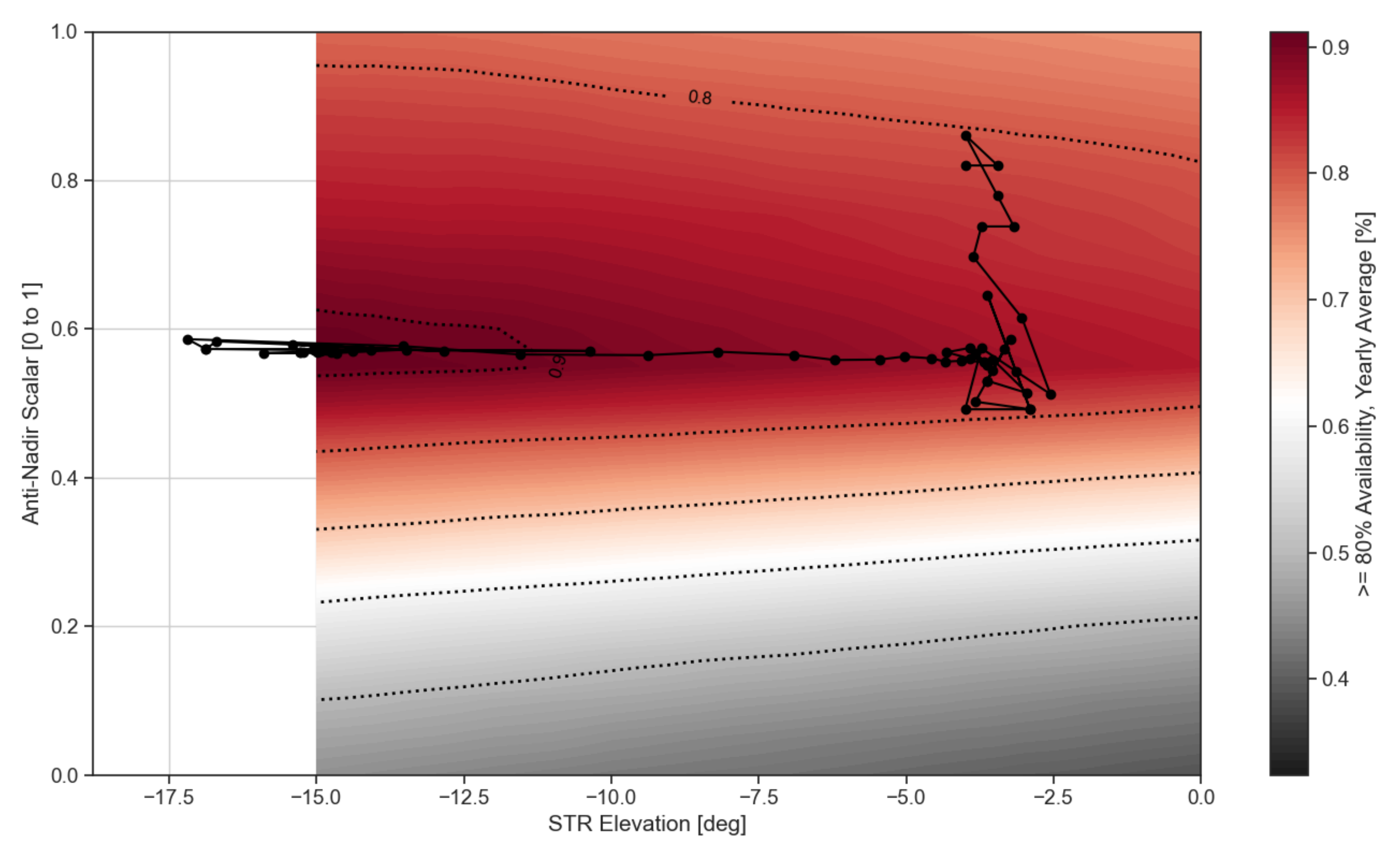

	Effectiveness (%)			
LTAN	10:00	11:00	15:05	21:00
Spring	93.20	94.30	87.70	87.40
Summer	89.65	87.20	82.65	82.65
Fall	93.10	95.10	87.70	88.30
Winter	97.00	97.60	95.60	95.70
Year	**93.25**	**93.60**	**88.45**	**88.55**
Average	**90.95**			

Mission 1

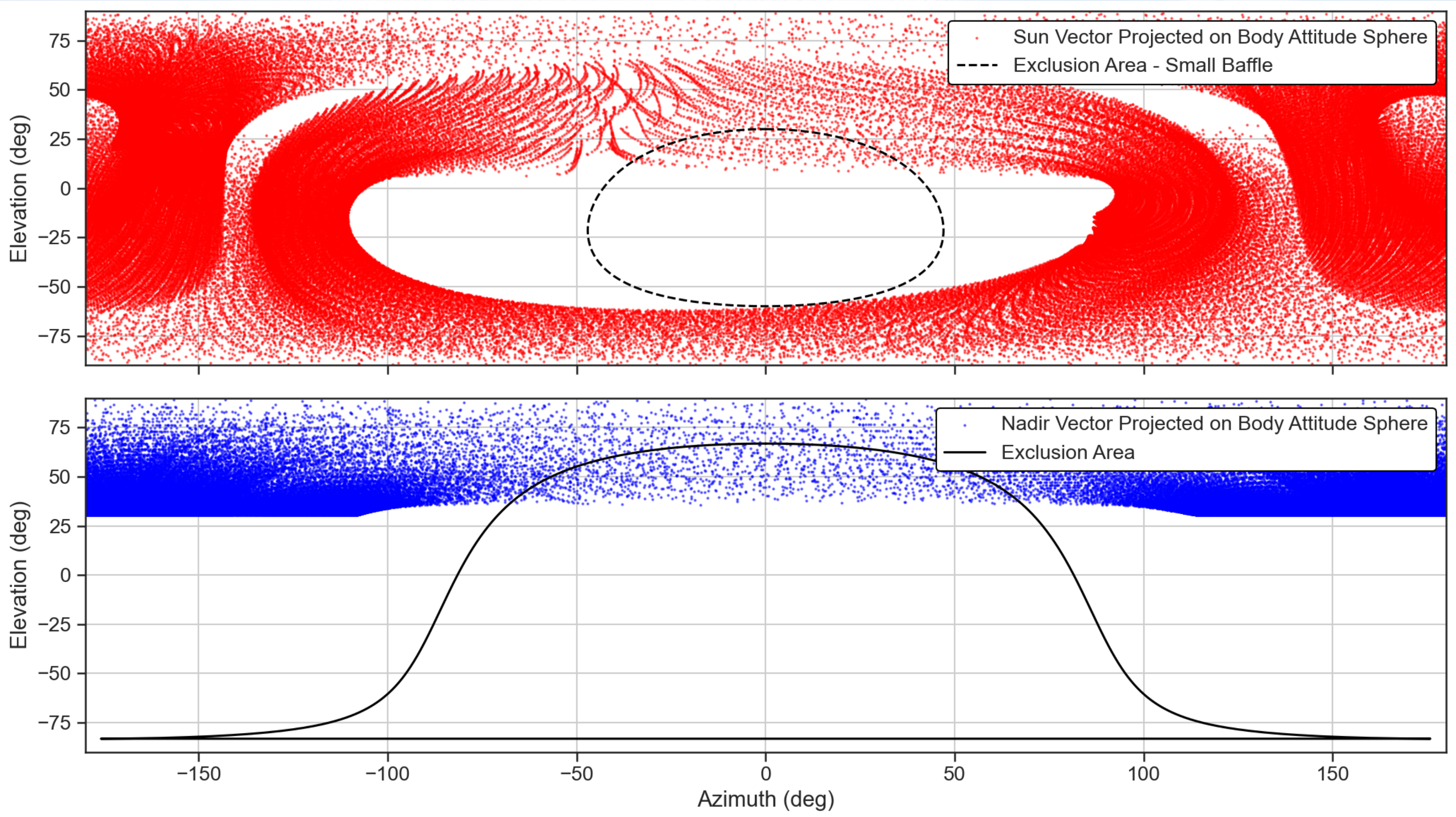
Sun Vector Projected on Body Attitude Sphere
Exclusion Area - Small Baffle
Nadir Vector Projected on Body Attitude Sphere
Exclusion Area
Elevation (deg)
Azimuth (deg)
75
50
25
0
−25
−50
−75
−150
−100
−50
0
50
100
150

Mission 1

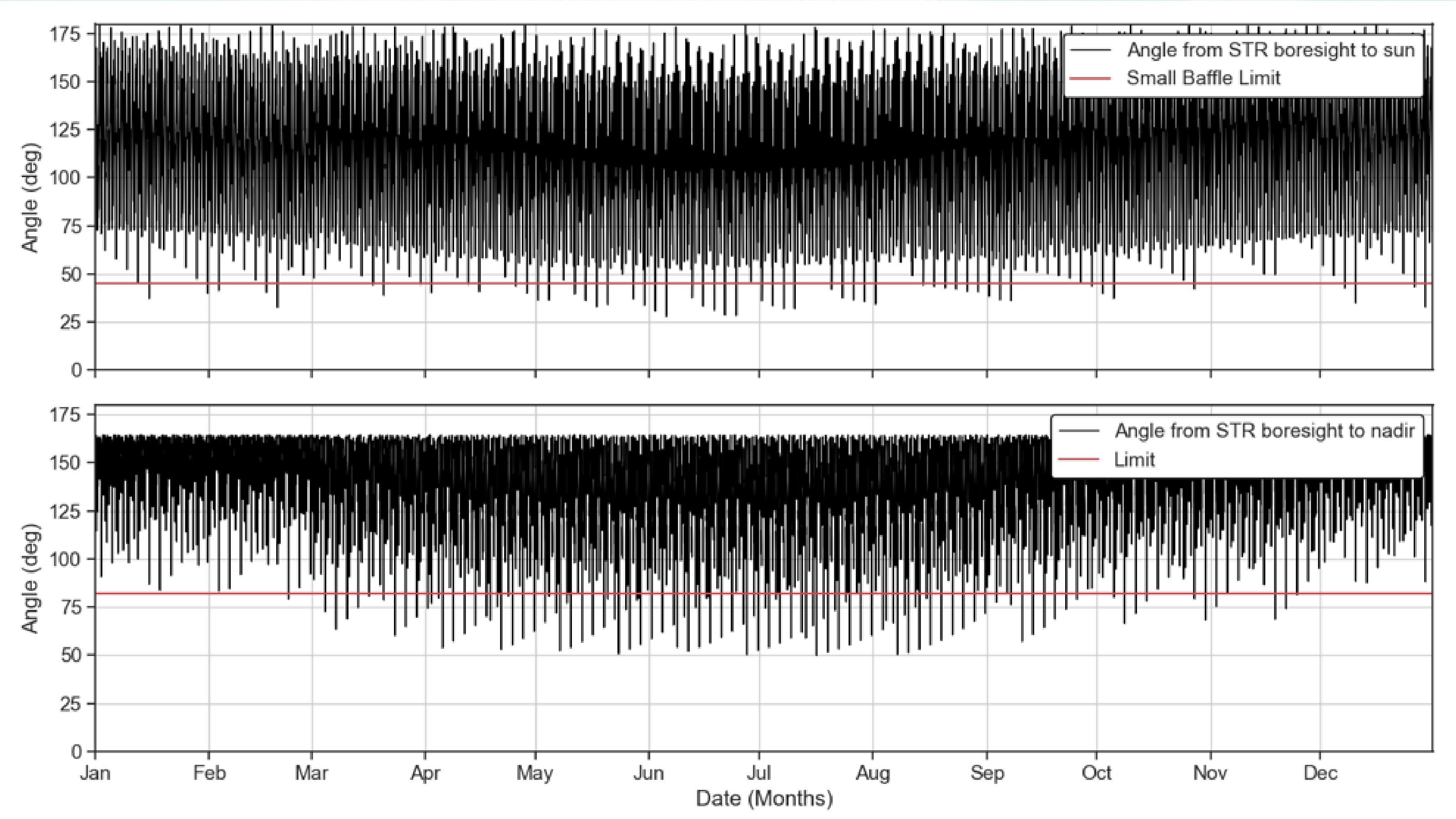
Angle from STR boresight to sun
Small Baffle Limit
Angle from STR boresight to nadir
Limit
Angle (deg)
175
150
125
100
75
50
25
0
Jan
Feb
Mar
Apr
May
Jun
Jul
Aug
Sep
Oct
Nov
Dec
Date (Months)

Mission 2

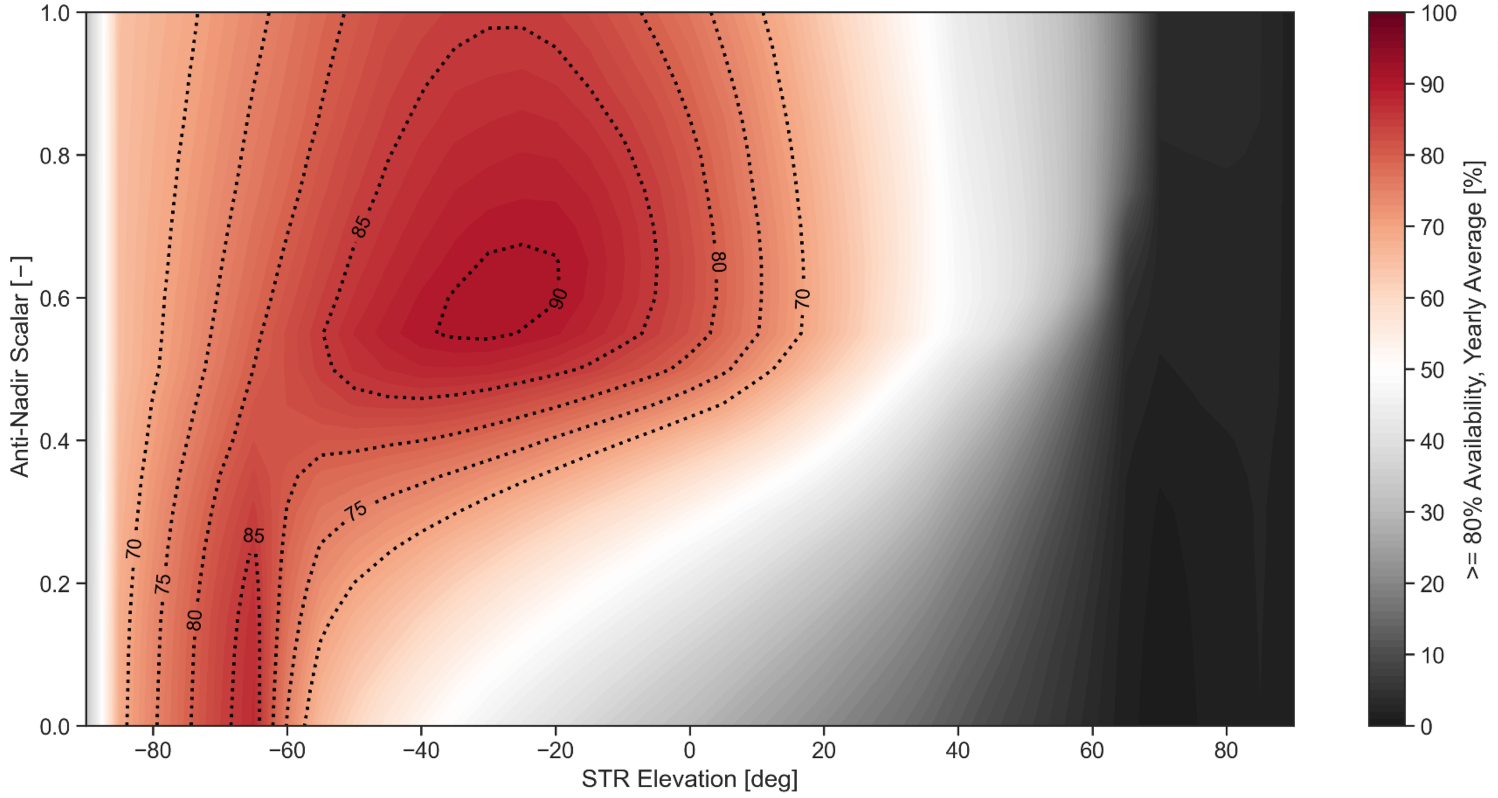

	Effectiveness (%)				
Orbit	6:00 LTAN	9:30 LTAN	11:00 LTAN	13:30 LTAN	42°
Spring	96.33	95.94	93.70	93.43	88.76
Summer	96.29	95.24	91.50	90.96	83.47
Fall	96.06	96.36	93.97	93.50	87.80
Winter	96.21	96.27	95.57	95.95	91.87
Year	**96.22**	**95.96**	**93.69**	**93.47**	**87.98**
Average			**93.46**		

Mission 2

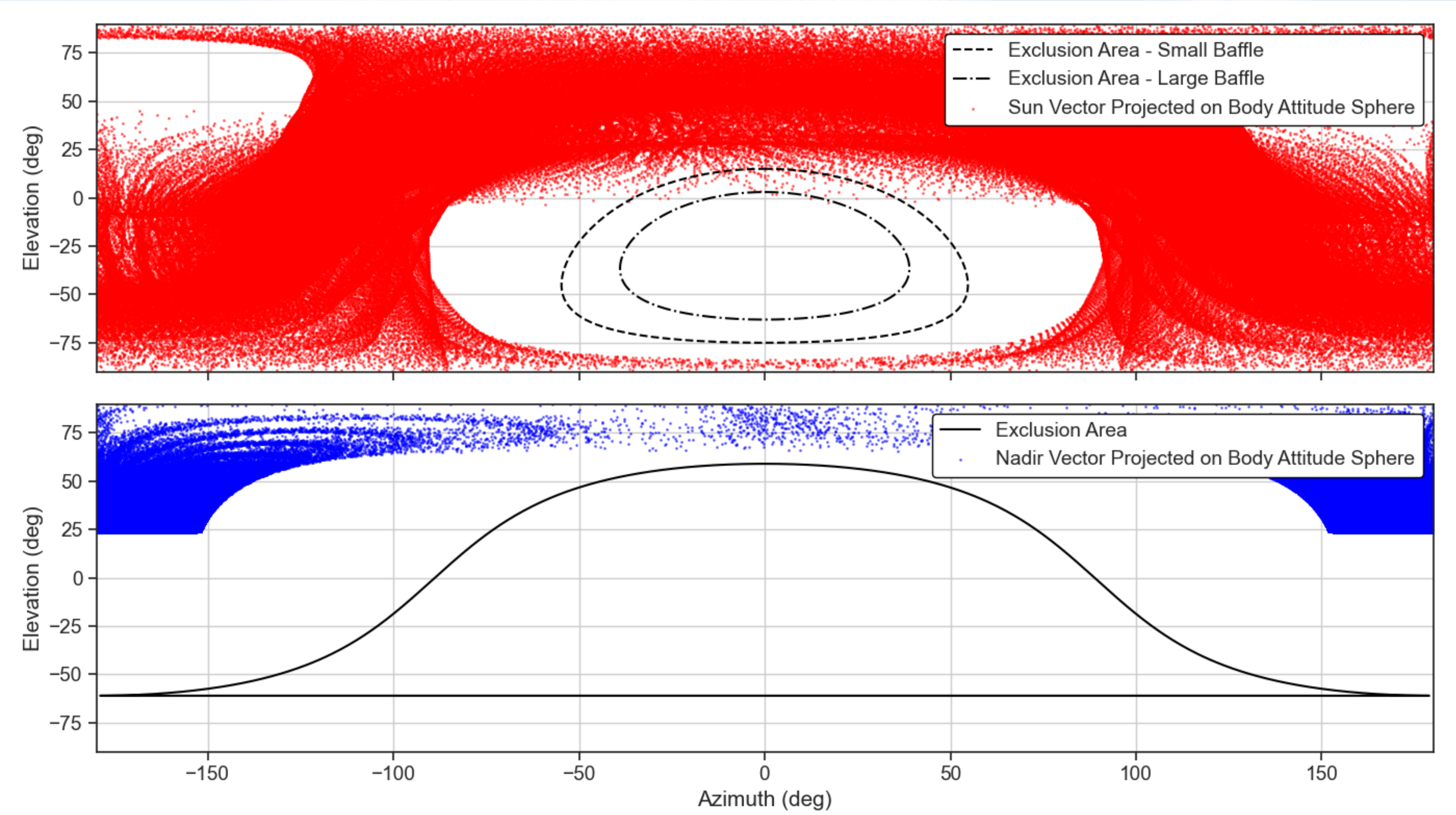
Exclusion Area - Small Baffle
Exclusion Area - Large Baffle
Sun Vector Projected on Body Attitude Sphere
Exclusion Area
Nadir Vector Projected on Body Attitude Sphere
Elevation (deg)
75
50
25
0
−25
−50
−75
−150
−100
−50
0
50
100
150
Azimuth (deg)

Mission 2

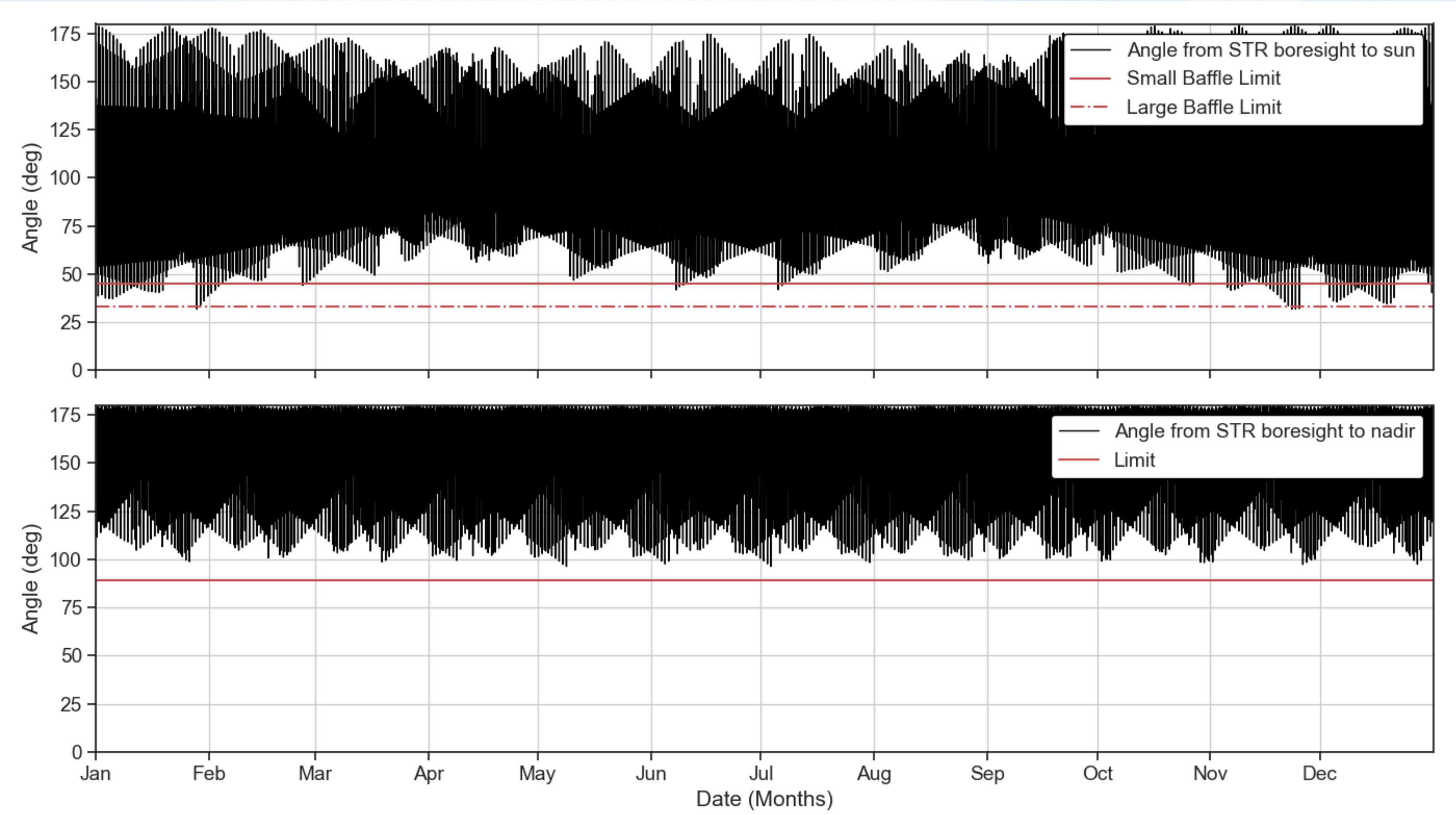
Angle from STR boresight to sun
Small Baffle Limit
Large Baffle Limit
Angle (deg)
175
150
125
100
75
50
25
0
Angle from STR boresight to nadir
Limit
Angle (deg)
Jan
Feb
Mar
Apr
May
Jun
Jul
Aug
Sep
Oct
Nov
Dec
Date (Months)

GNC System Simulations

- Sample mission using DEFIANT platform based on real mission
- Earth observation mission with altitude between 550 km and 650 km, SSO orbit with no LTAN constraints
- Area of interest is the maritime geographical area NAVAREA XIX and ground station at The Hague

Operational Mode	Description
Limb-Pointing	Align Yagi antenna towards a target with some angle above or below Earth limb. Spacecraft sweeps across the target area to maximize coverage.
Coarse Target Tracking	Ground target tracking with UHF antenna.
Fine Target Tracking	Ground target tracking with optical payload boresight with star tracker constraint.

UTIAS SFL

Simulation Configuration

- 550 km altitude chosen for all simulations
  - Providing worst-case star tracker obscuration from Earth's limb and worst-case eclipse fraction
- LTANs of 00:00, 03:00 and 06:00 were chosen
  - Covering the range of ground lighting conditions
- All simulation cases were run at both the summer and winter solstice, as these epochs result in the most extreme illumination conditions
  - Summer solstice: worst-case Sun angle for star tracker during high-latitude observations
  - Winter solstice: large portions of the passes over the area of interest occurring in eclipse

UTIAS SFL

Limb Pointing

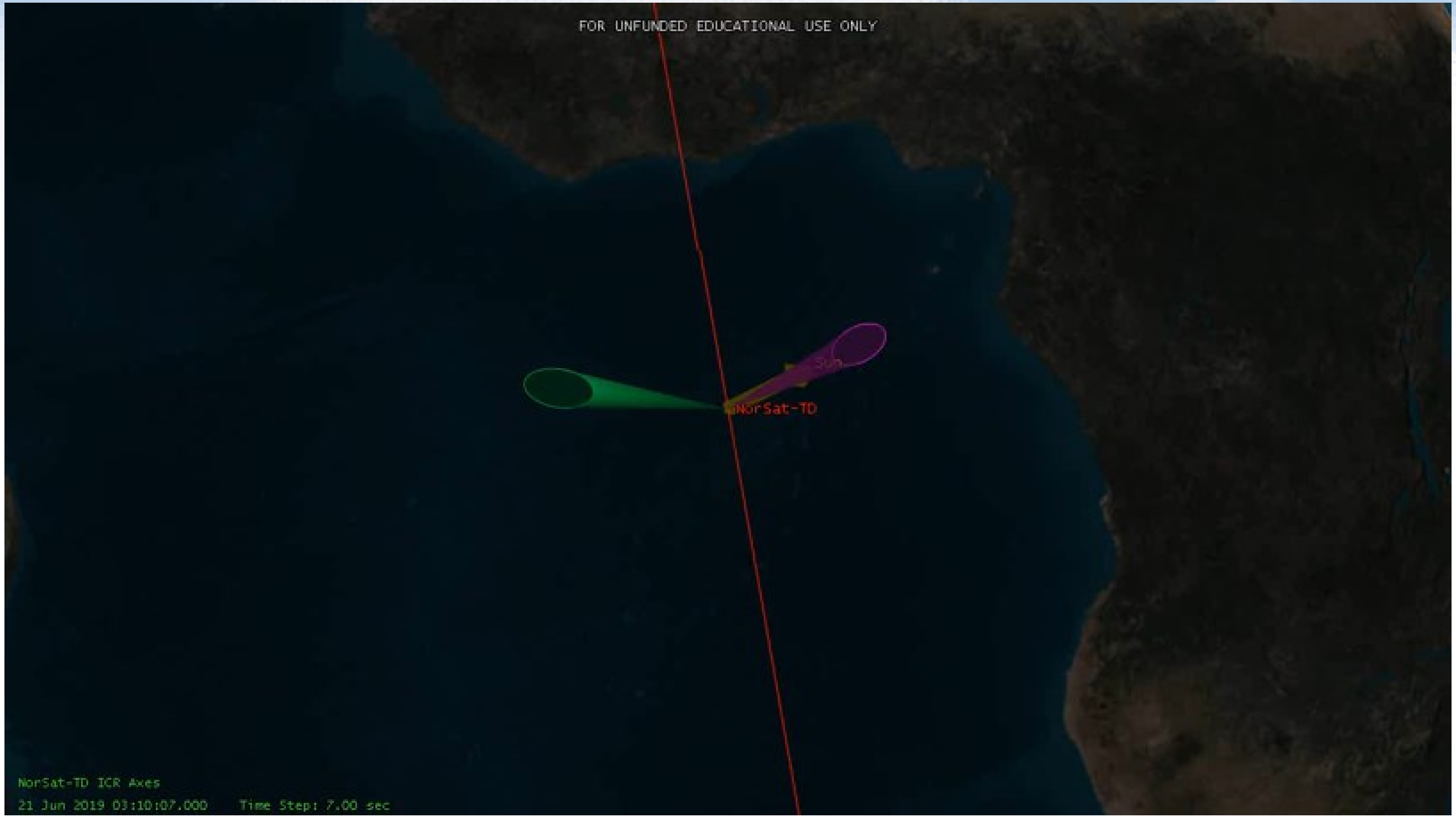

https://youtu.be/h23ajHFMelE

Limb Pointing

- **Requirement:**
  - When in limb pointing mode,
    - the pointing accuracy shall be 7° RMS, or better
    - the rate accuracy shall be 3°/s RMS, or better

Epoch	LTAN	$\lvert\phi_e\rvert$ (°)	$\lvert\boldsymbol{\omega}_e\rvert$ (°/s)
Summer Solstice	00:00	3.549	0.019
Summer Solstice	03:00	1.973	0.010
Summer Solstice	06:00	1.703	0.008
Winter Solstice	00:00	4.236	0.012
Winter Solstice	03:00	4.893	0.010
Winter Solstice	06:00	5.451	0.012

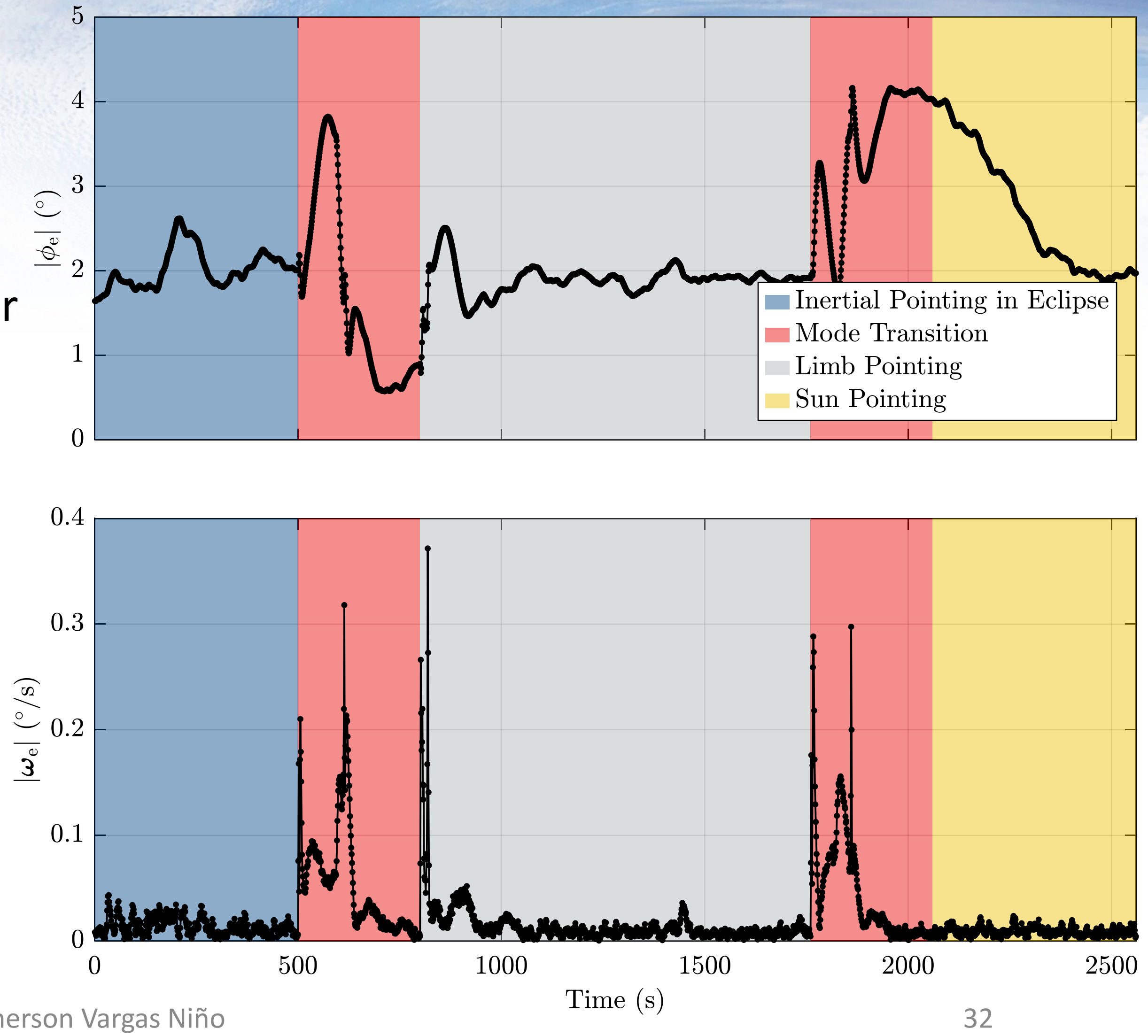

Coarse Target Tracking

https://youtu.be/y_MSQMQBxls

Coarse Target Tracking

- **Requirement:**
  - When in coarse target tracking mode,
    - the pointing accuracy shall be 10° 2σ, or better
    - the rate accuracy shall be 1°/s 2σ, or better

Epoch	LTAN	$\lvert\phi_e\rvert$ (°)	$\lvert\boldsymbol{\omega}_e\rvert$ (°/s)
Summer Solstice	00:00	6.818	0.065
Summer Solstice	03:00	2.809	0.049
Summer Solstice	06:00	2.116	0.030
Winter Solstice	00:00	4.949	0.032
Winter Solstice	03:00	5.120	0.038
Winter Solstice	06:00	5.329	0.033

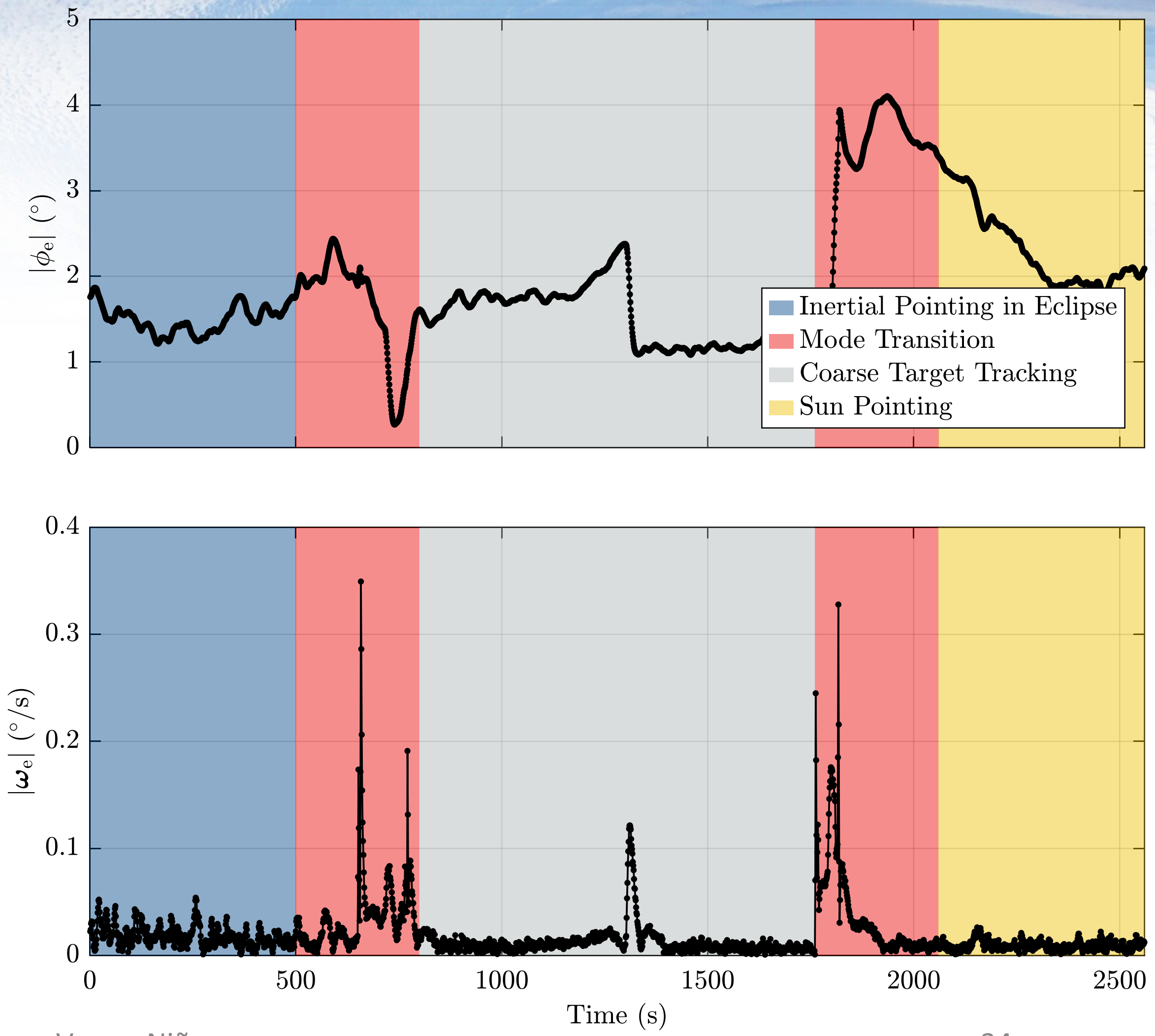

Fine Target Tracking

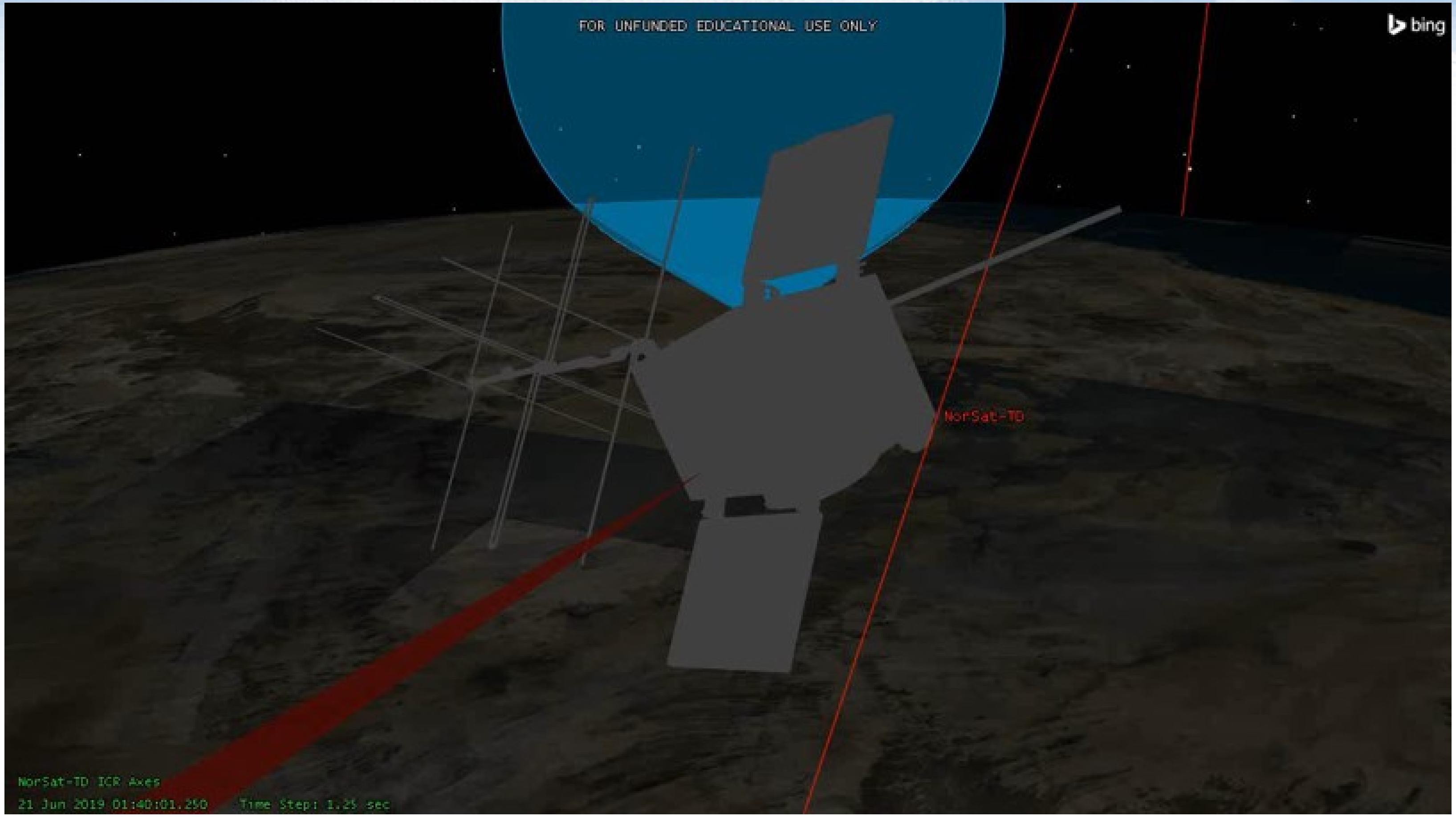

https://youtu.be/4d8PfNCmtak

Fine Target Tracking

- **Requirement:**
  - When in fine target tracking mode,
    - the pointing accuracy shall be 0.5° 2σ, or better
    - the rate accuracy shall be 0.14°/s 2σ, or better

Using weighted sum constraint

Epoch	LTAN	$\lvert\phi_e\rvert$ (°)	$\lvert\boldsymbol{\omega}_e\rvert$ (°/s)
Summer Solstice	00:00	0.052	0.211
Summer Solstice	03:00	0.242	0.895
Summer Solstice	06:00	0.046	0.163
Winter Solstice	00:00	0.072	0.233
Winter Solstice	03:00	0.404	1.161
Winter Solstice	06:00	0.474	1.941

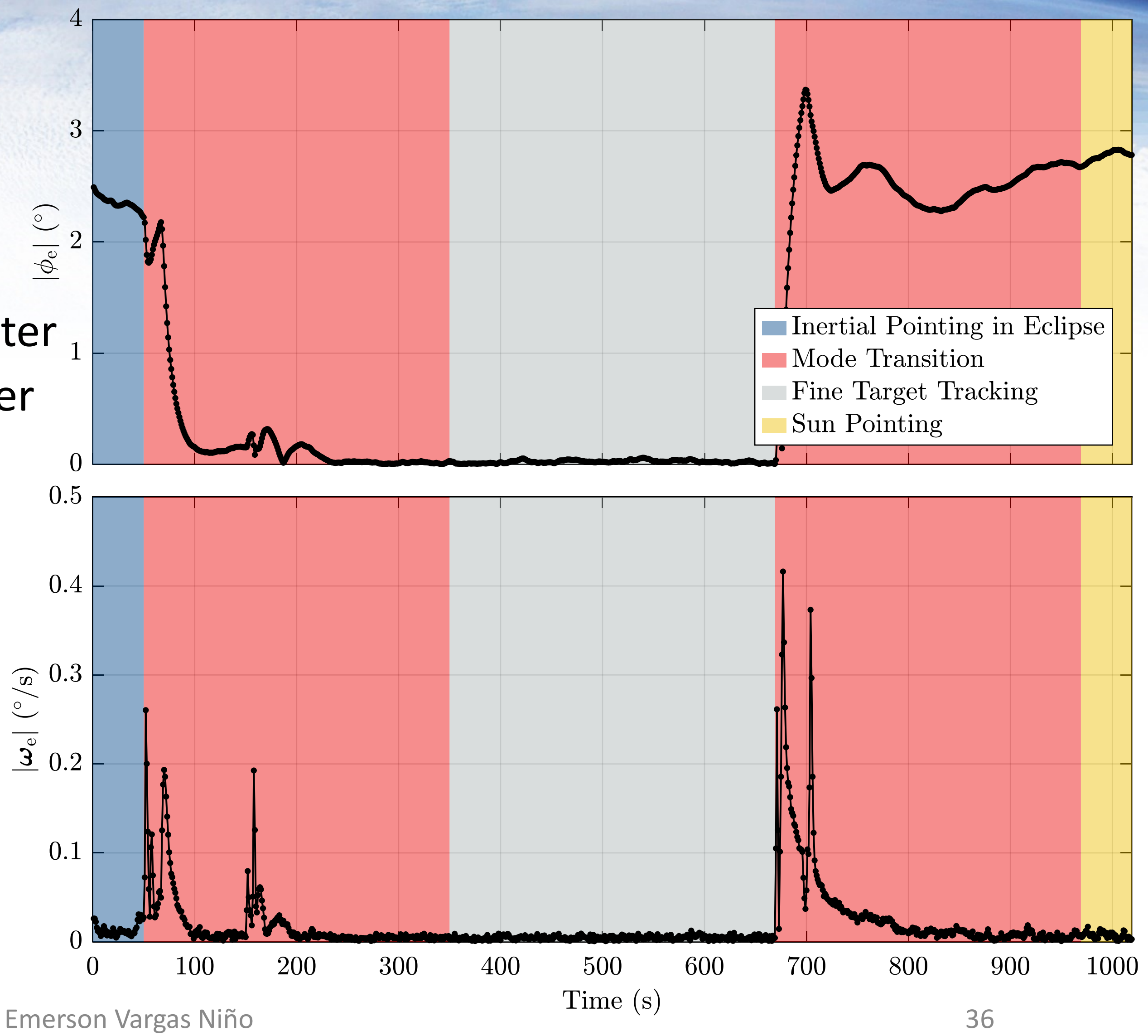

Propulsion System

UTIAS SFL

Propulsion Systems at SFL

- Used mainly to control the relative orbit in formation flying missions
- **Previously:** Monopropellant thruster developed; 3 design iterations
  - Final thruster lifetime of 50.3 hours, exceeding 43.1 hour requirement
  - components were varied resulting in increased performance in one aspect, at the cost of decreased performance in another
  - Test campaign highlighted issues related to thruster lifetime, heater placement, reignition temperature and localized catalyst deactivation
- Methods to further improve efficiency, lifetime and consistent performance can continue to be explored to improve the system for future implementation

Monopropellant Thruster

- A monopropellant system operates through the exothermic decomposition of a propellant resulting in hot gases, which are accelerated through a nozzle

- Decomposition can be brought on by heating propellant or passing propellant through catalyst, providing **low energy pathway to decomposition**
  - In the case of N_2O, the decomposition reaction is given by,

$$\mathrm{N_2O} \rightarrow \mathrm{N_2} + \frac{1}{2}\mathrm{O_2} - 82\,\frac{\mathrm{kJ}}{\mathrm{mol}}$$

SFL Monopropellant Thruster

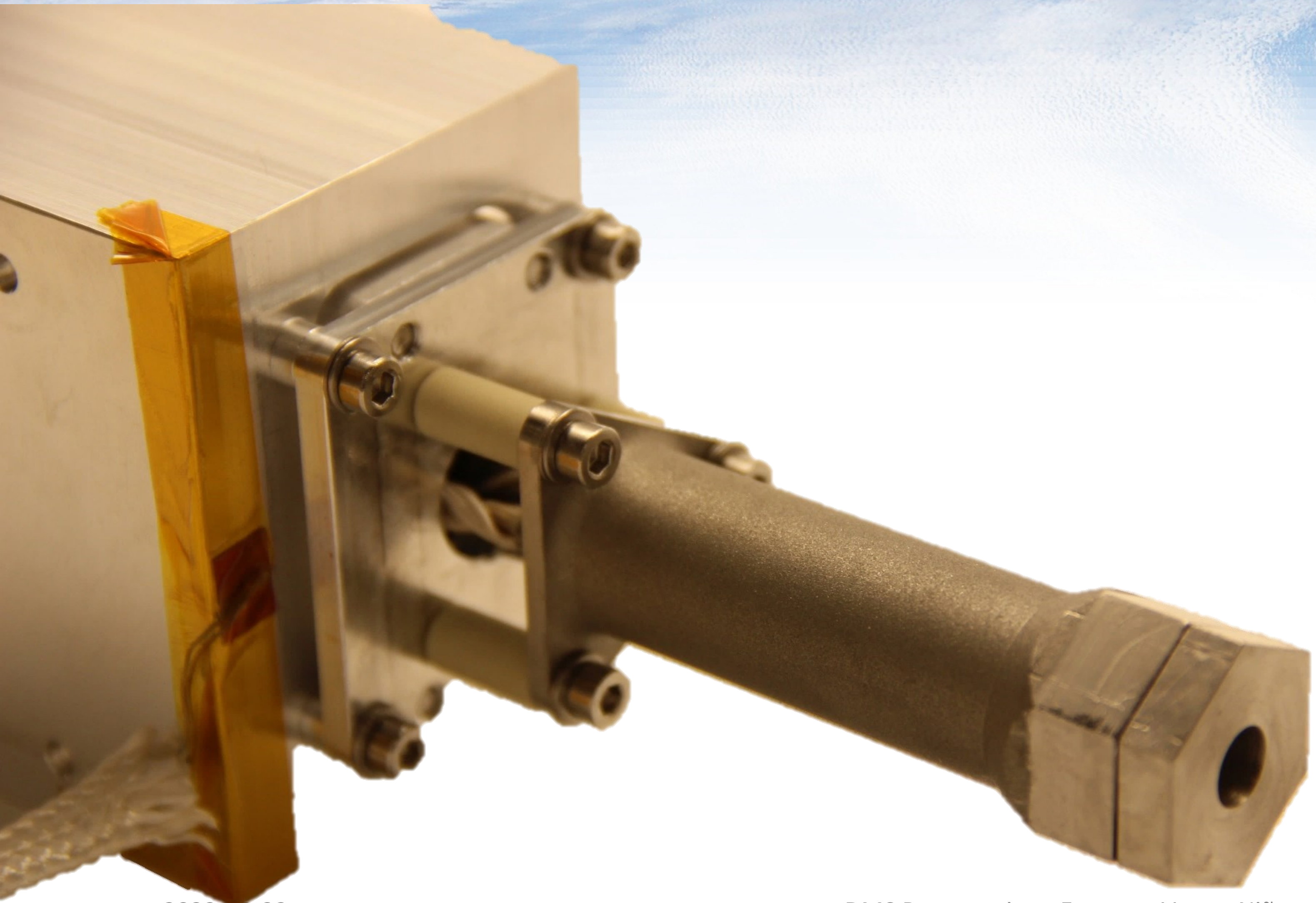

SFL Monopropellant Thruster

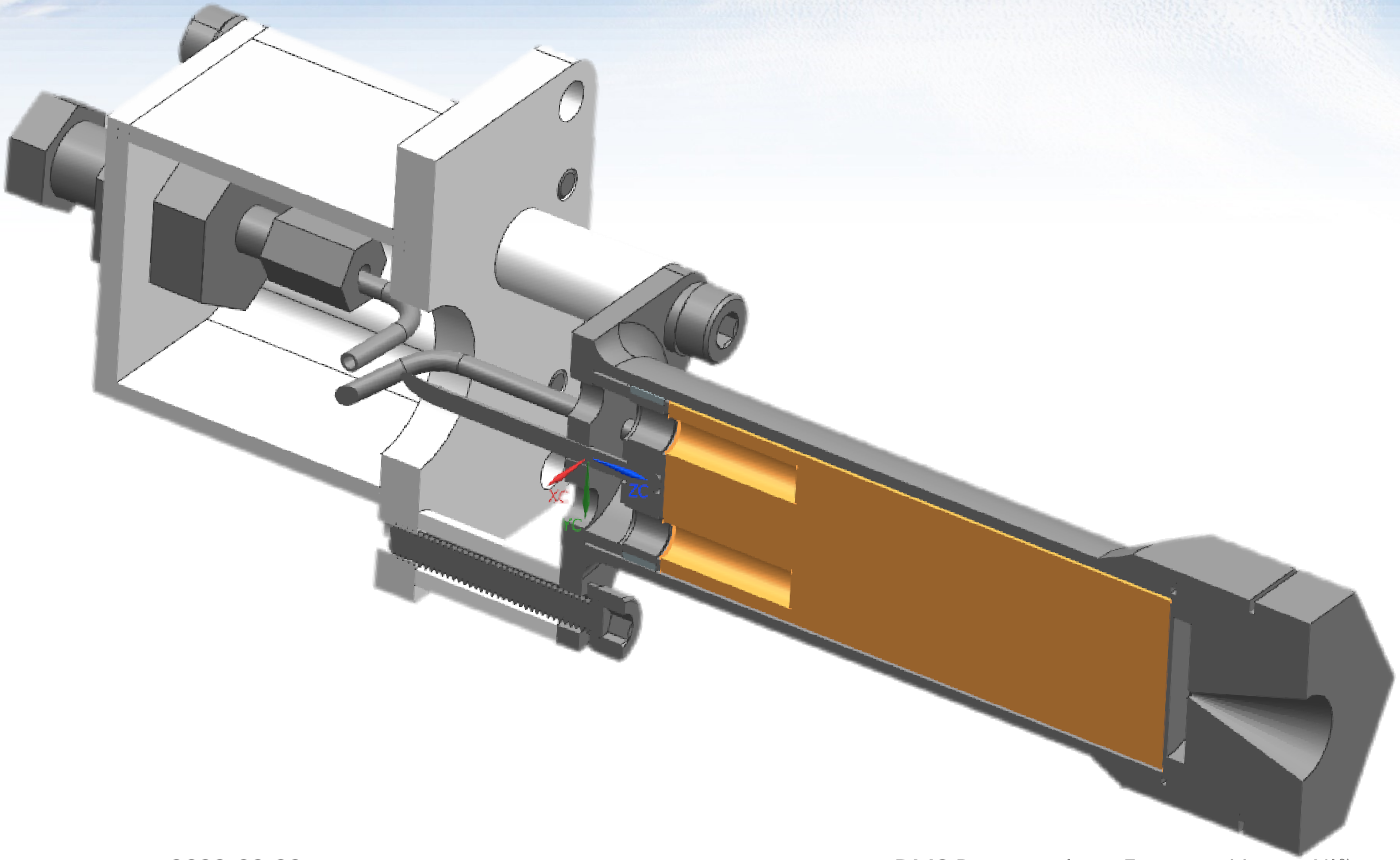

Monopropellant Thruster Investigation

- Thermal Sintering
  - Surface area of catalyst carrier decreases as temperature increases
  - Decrease in surface area leads to decrease in catalytic activation
  - System temperature can be modeled with transient control volume approach
- Packed Bed Ordering Effect
  - Presence of chamber wall causes ordering effect on particles near the wall
  - Results in preferential flow paths in the catalyst bed leading to localized deactivation

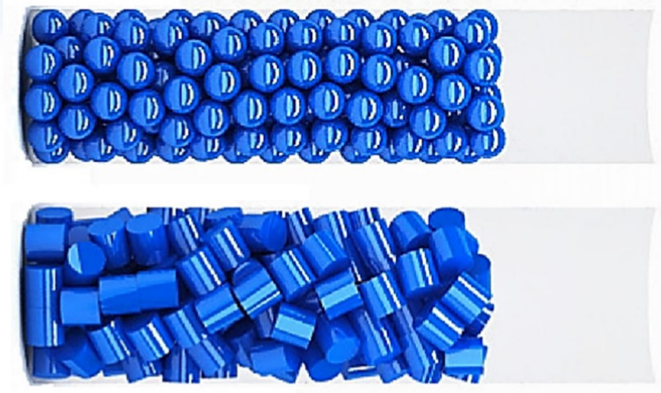

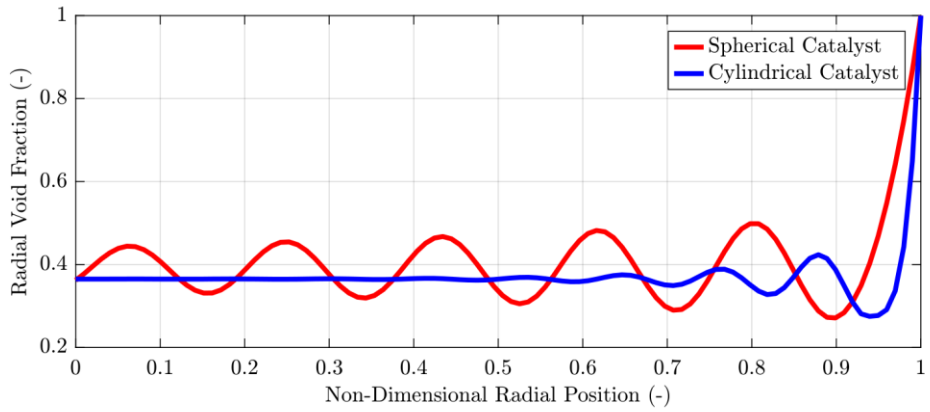

Monopropellant Thruster Investigation

- Injection
  - Poorly atomized propellant injected into thrust chamber can cause large localized thermal loads along catalyst bed leading to shortened lifetime
- Chamber Length
  - There is an ideal chamber length which maximizes temperature entering the nozzle leading to highest thrust, specific impulse
  - Shorter lengths mean propellant not fully decomposed, longer length means losing energy heating catalyst bed and chamber walls
  - Ideal chamber length can be found numerically, using 1D steady-state flow models

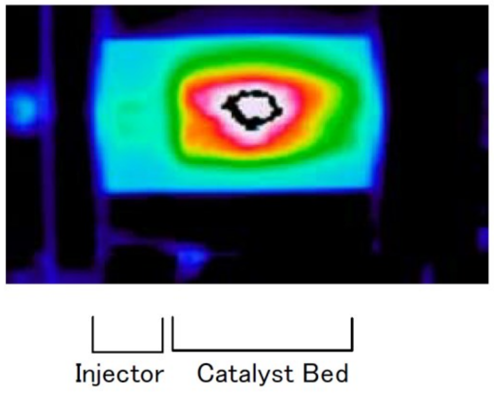

(a) The old 1N thruster design Injector

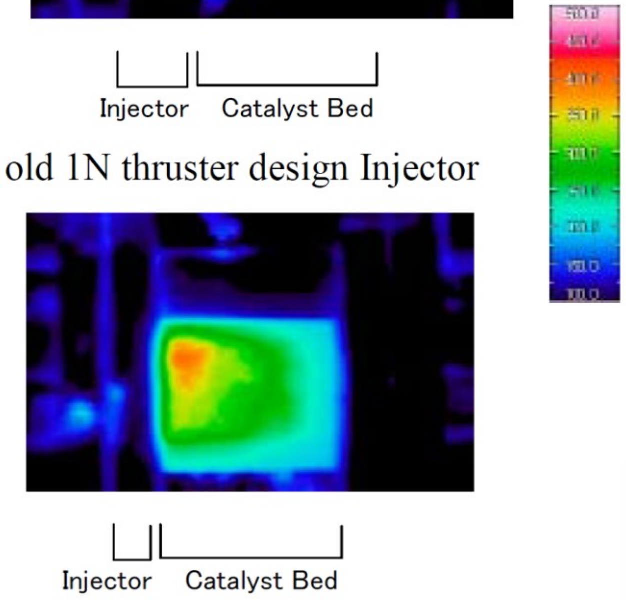

(b) The newly selected design Injector

Source: Go FUJII, “The Development Results Of The Long Life 1 N Hydrazine Monopropellant Thruster”

Deployable Solar Panel System

Deployable Solar Panel System

- Power generation and launch volume requirements motivate the use of deployable solar panels for DEFIANT → first hinged deployable system
  - Two symmetric solar wings simplify analysis and mechanical design
  - Low impact on bus layout due to high clearance from bus
  - Held down with pre-load force
- Test campaign and modifications raised technology readiness level from 3 to 9
- 100% success rate 24 different panels across 12 spacecraft

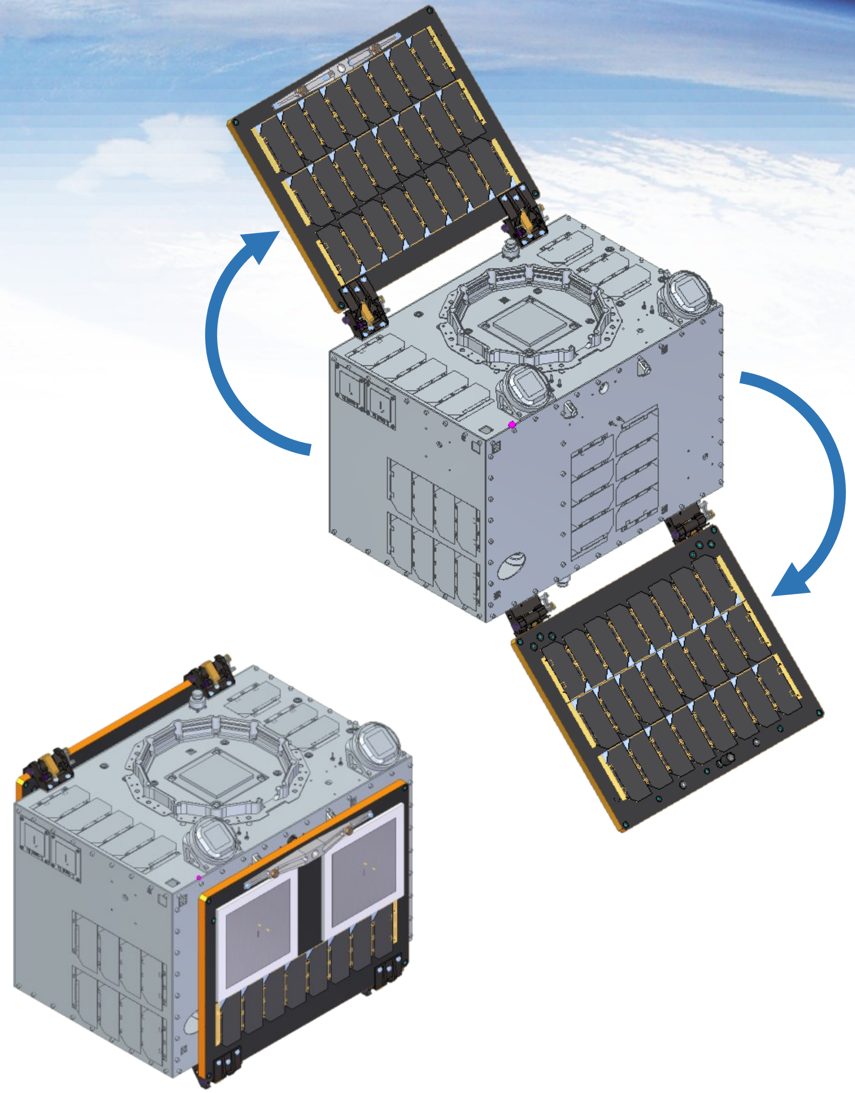

Main Components

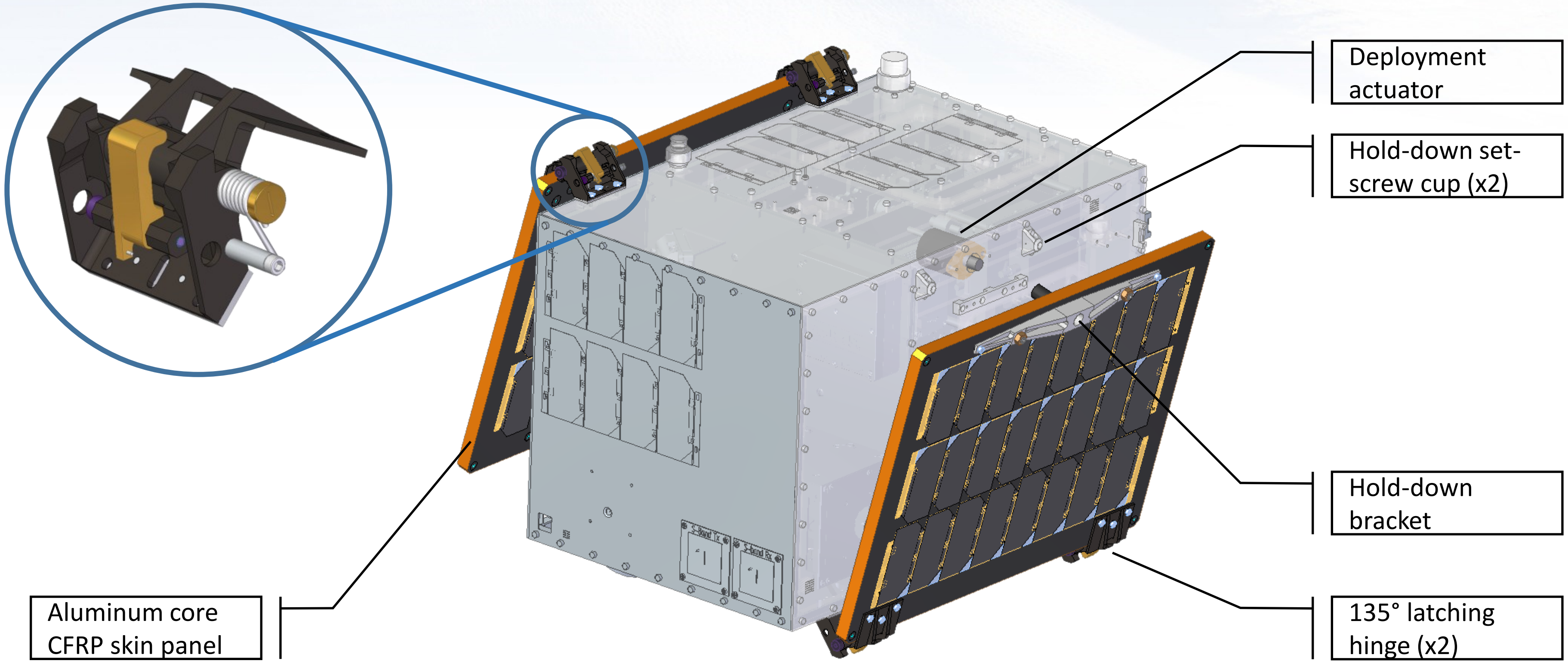

Hinge Motion – Section View

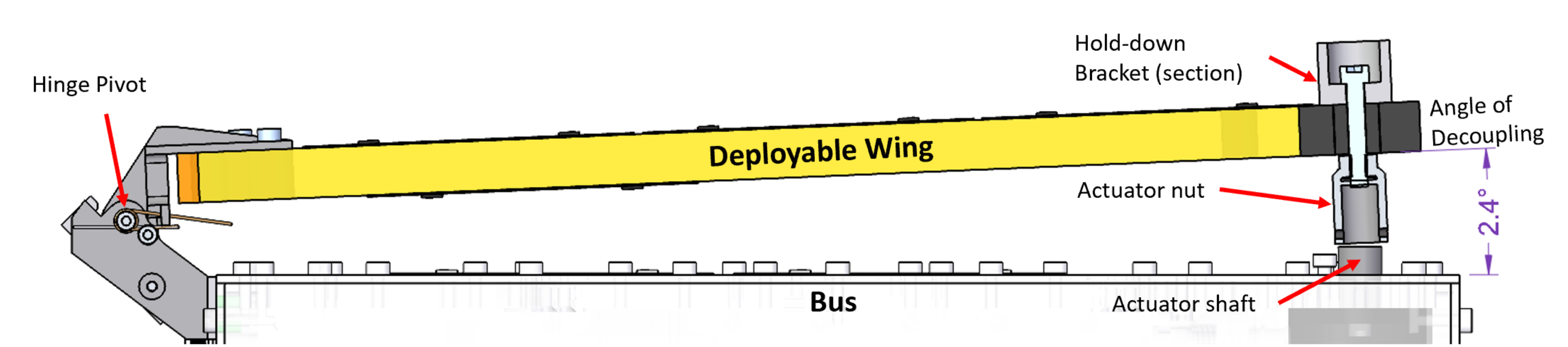

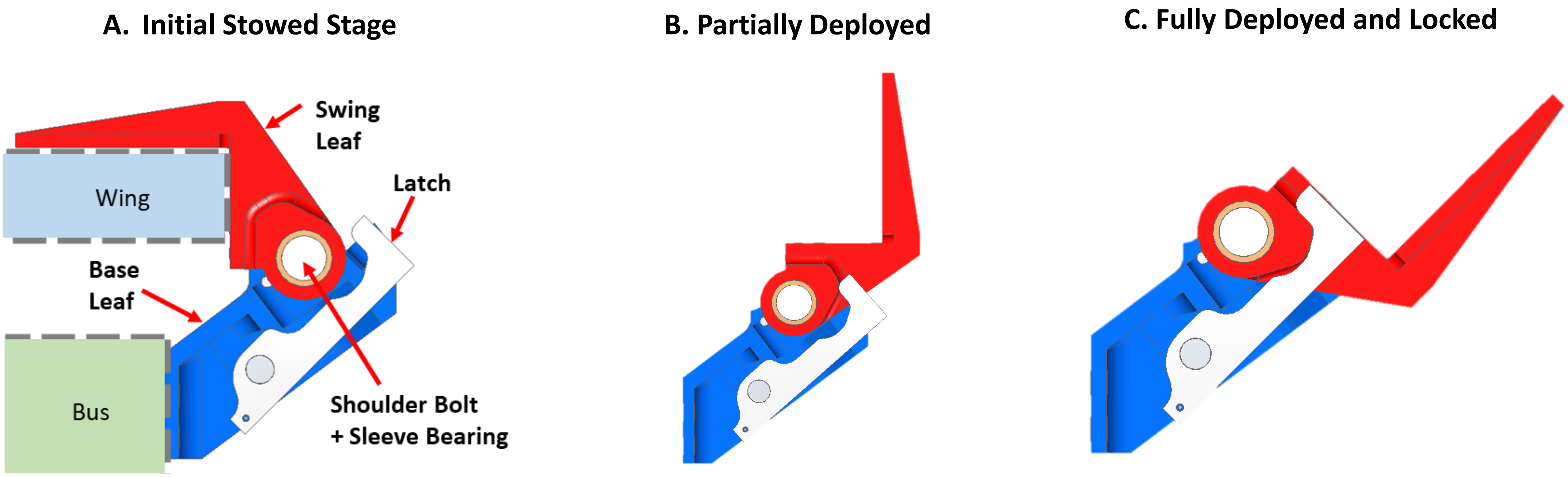

Test Campaign

- Three-stage test campaign on deployable solar panel system:
  - **Pre-Qualification:** de-risk this technology by testing it in a variety of conditions and adjusting different design parameters. Includes:
    1. Bench Tests: Verify basic deployment functionality, validate analytical assumptions
    2. Thermal Test: Evaluate min/max temperature effects in thermal chamber
    3. TVAC Test: Verify and characterize deployment in vacuum
    4. Vibration Test: Mounted on structure during structural qualification test
  - **Qualification:** tested beyond its nominal environmental operating conditions, ensuring there is sufficient margin in the design
  - **Acceptance:** unit-level testing, prior to integration into spacecraft, and system-level testing, complete spacecraft testing, following its construction

UTIAS SFL

Test Setup and GSE

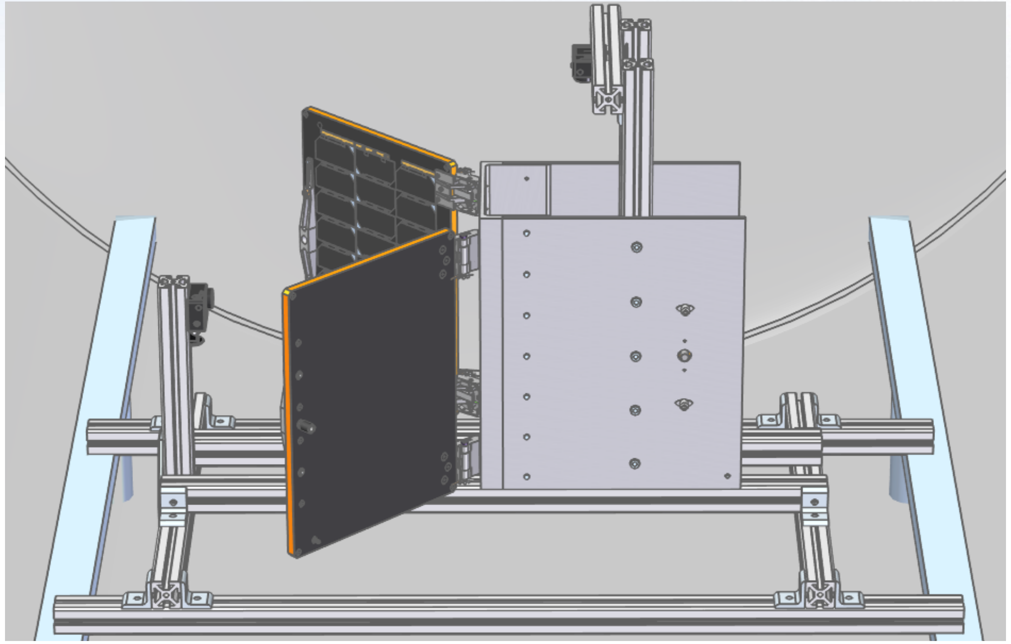

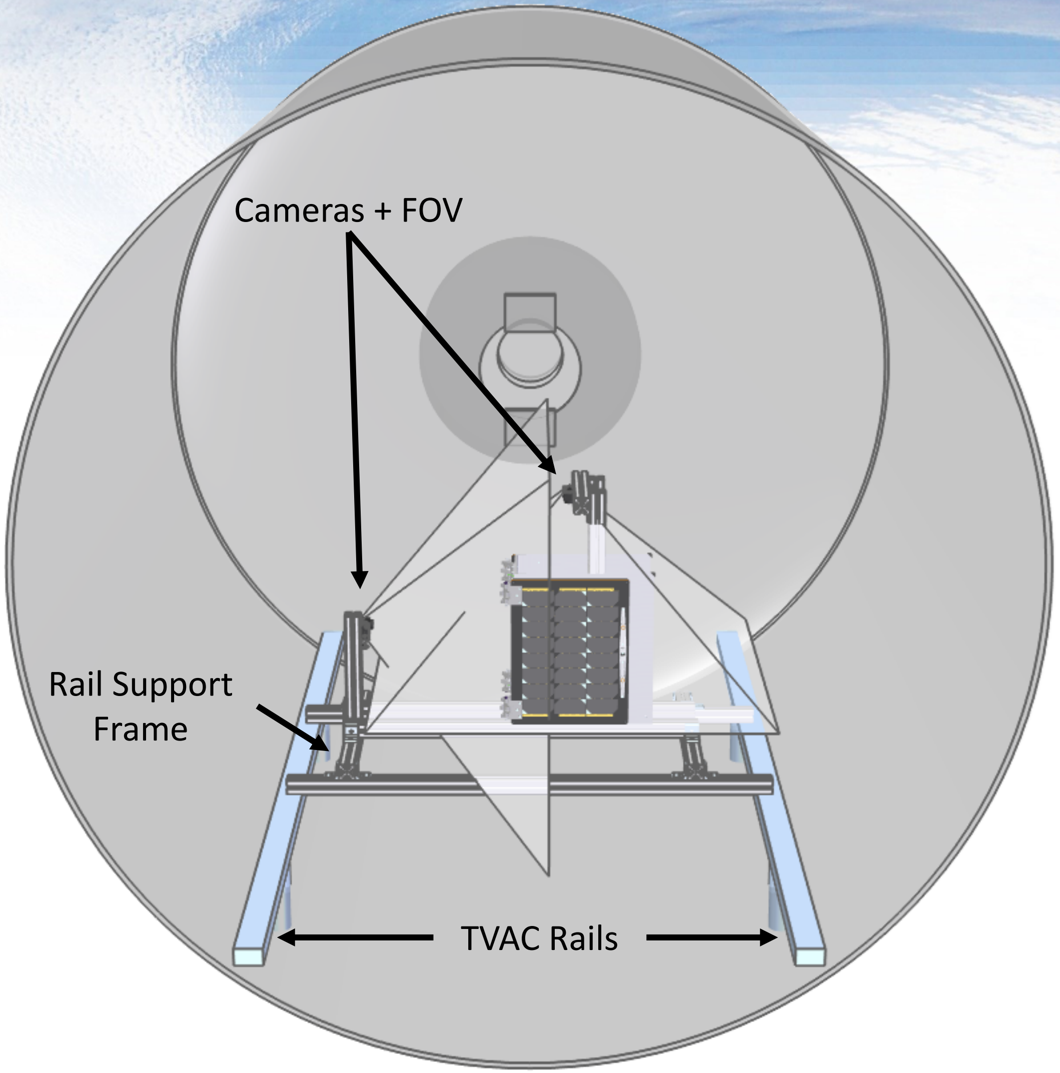

Test Setup and GSE

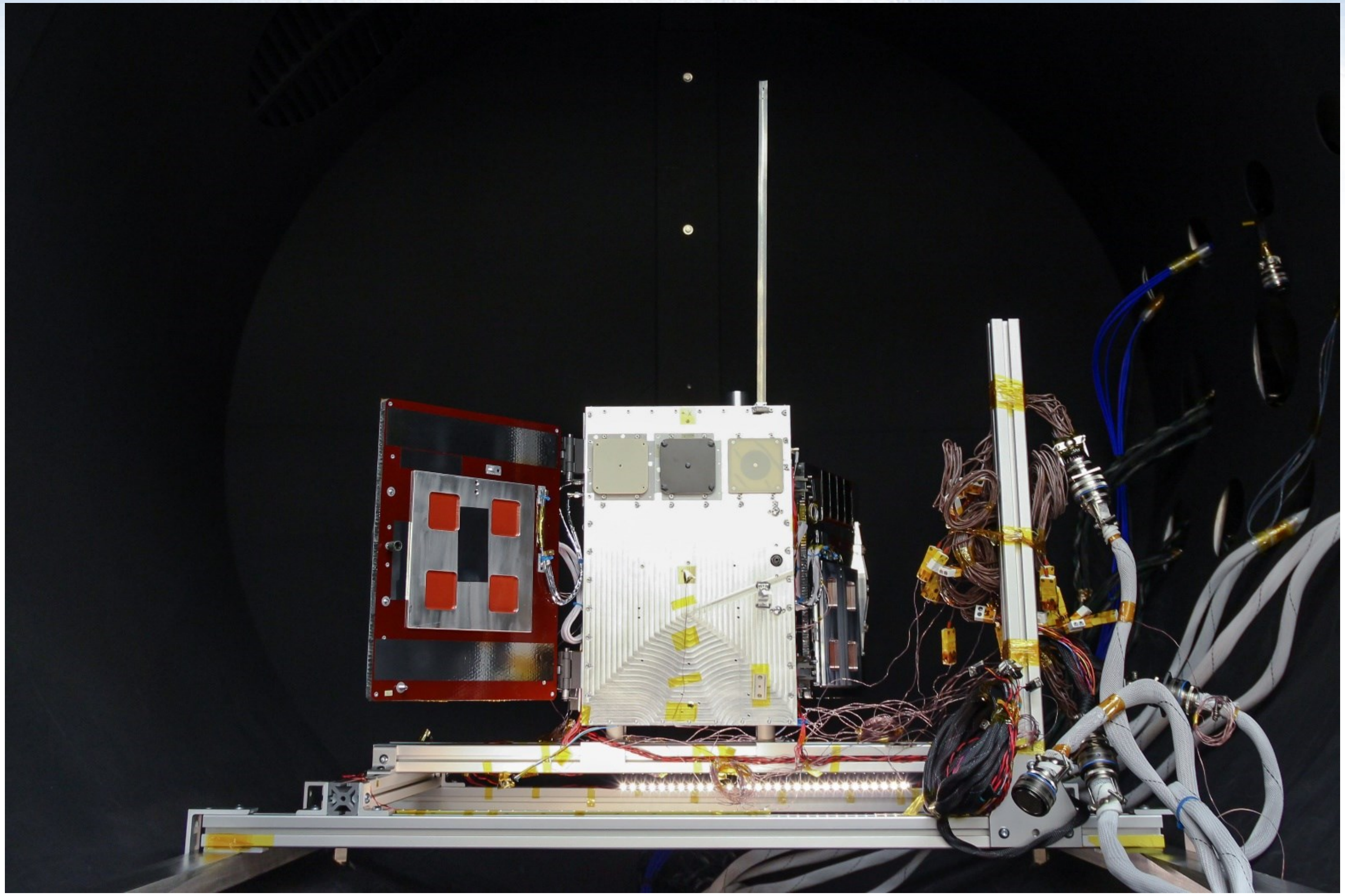

Vacuum Deployment - Top-Down Camera

https://youtu.be/L4eWddo0feE

Partial deployment in TVAC

https://youtu.be/Pu7WYwUrJHE

Deployment Condition	Result	Panel-Bus Gradient During Deployment [°C]
Cold	Did latch	84.6
Hot	Did not latch	139.2

Partial deployment in TVAC - Causes

- Differential thermal expansion analysis predicts interference at temperature gradient experience during TVAC hot deployment
  - **Axial interference** in the space between hinge swing leaf and hinge base leaf
  - **Radial interference** in the space between shoulder bolt and sleeve bearing
- TVAC Panel-Bus gradient for hot deployment was far greater than:
  - Predicted by thermal simulations and margin
  - Calculated value which would result in non-successful deployment

	Panel-Bus Temperature Gradient [°C]
Temperature gradient predicted by FEA on orbit	60
Temperature gradient seen in TVAC	139.2

Partial deployment in TVAC - Causes

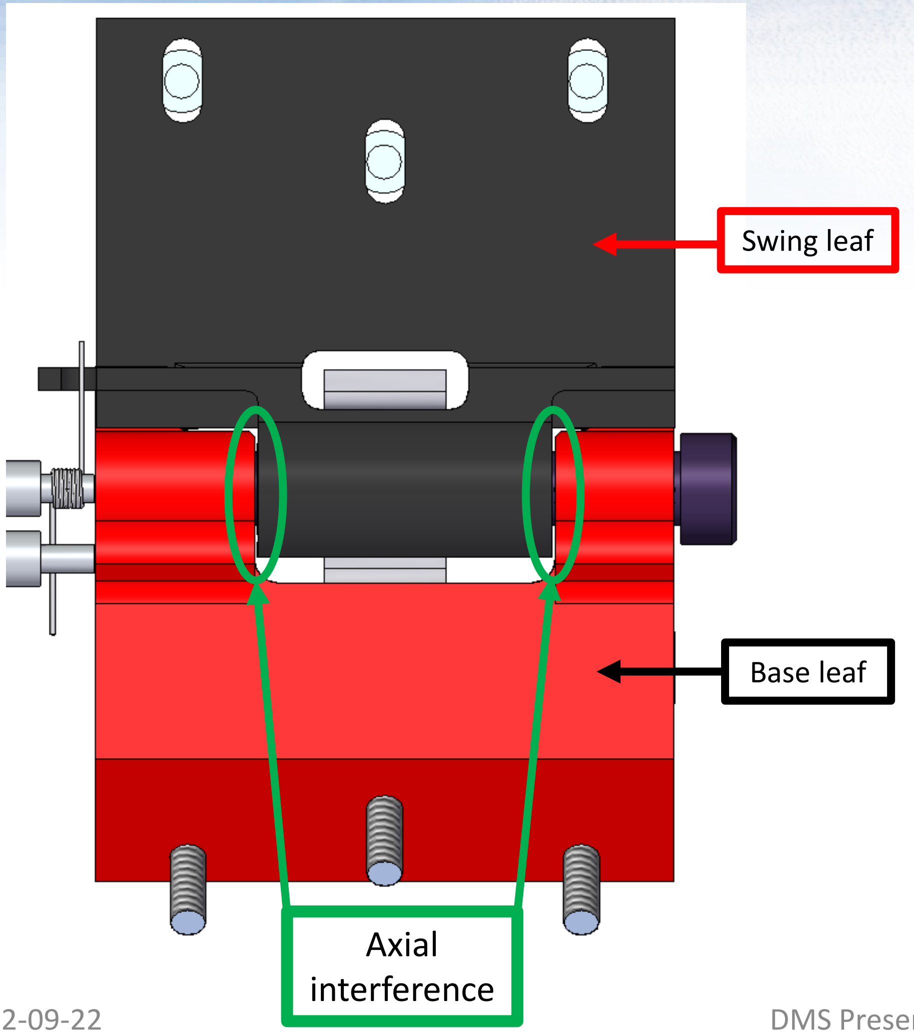

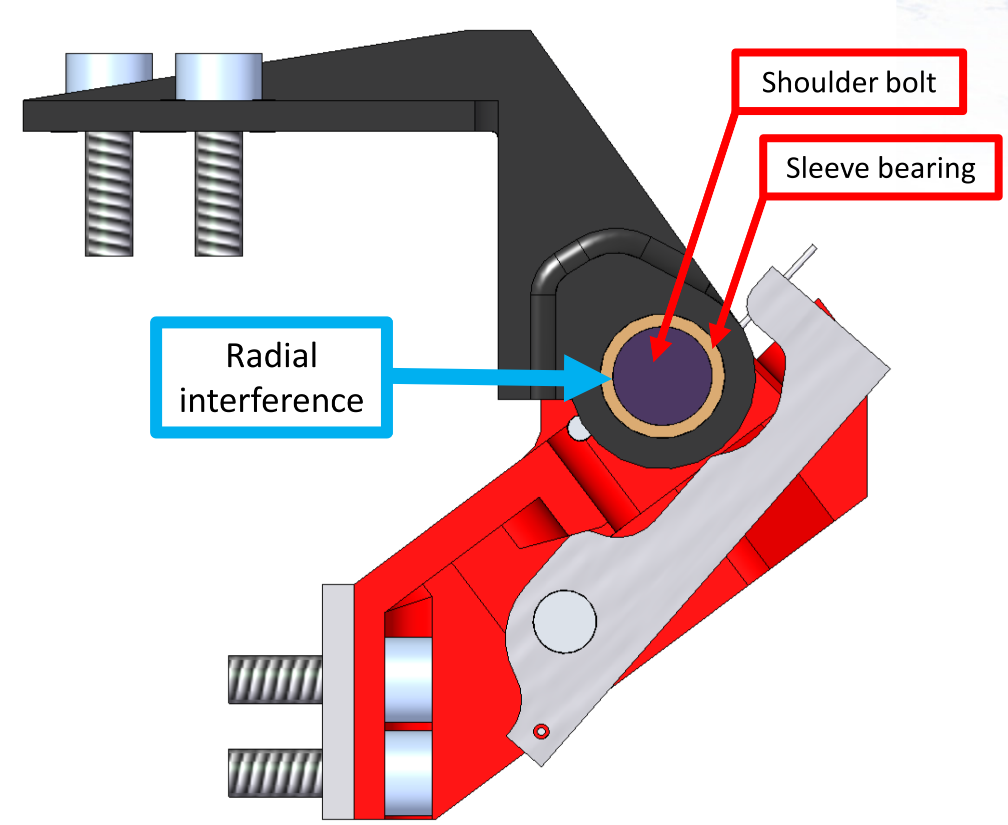

UTIAS SFL

Recreating TVAC partial deployment

- Recreated TVAC thermal conditions that lead to partial deployment, in thermal chamber
- Restrictions to the achievable gradient, due to convection, led to targeting half the gradient while reducing clearances by half
- Axial and radial clearances were reduced via installation of axial and radial shims

Linear Thermal Expansion Equation

$$\Delta L = \alpha_L L_0 \Delta T$$

$$\frac{\Delta L}{2} = \alpha_L L_0 \frac{\Delta T}{2}$$

$\Delta L = \text{Change in length}$

$\alpha_L = \text{Coefficient of linear thermal expansion}$

$L_0 = \text{Original length}$

$\Delta T = \text{Change in temperature}$

Recreating TVAC partial deployment

Installed:

- Two patch heaters on dummy bus (U-Channel) to create a large wing-to-bus thermal gradient
- Axial and radial shims to reduce axial and radial clearances
- Wing harnesses to simulate bending stiffness

Patch heater

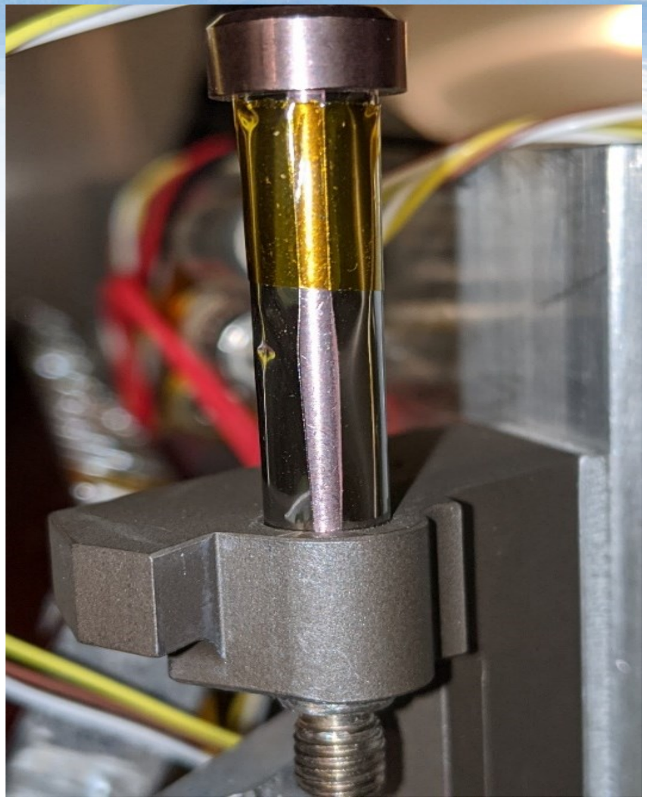

Radial shim installation

Thermal Chamber Deployment Test

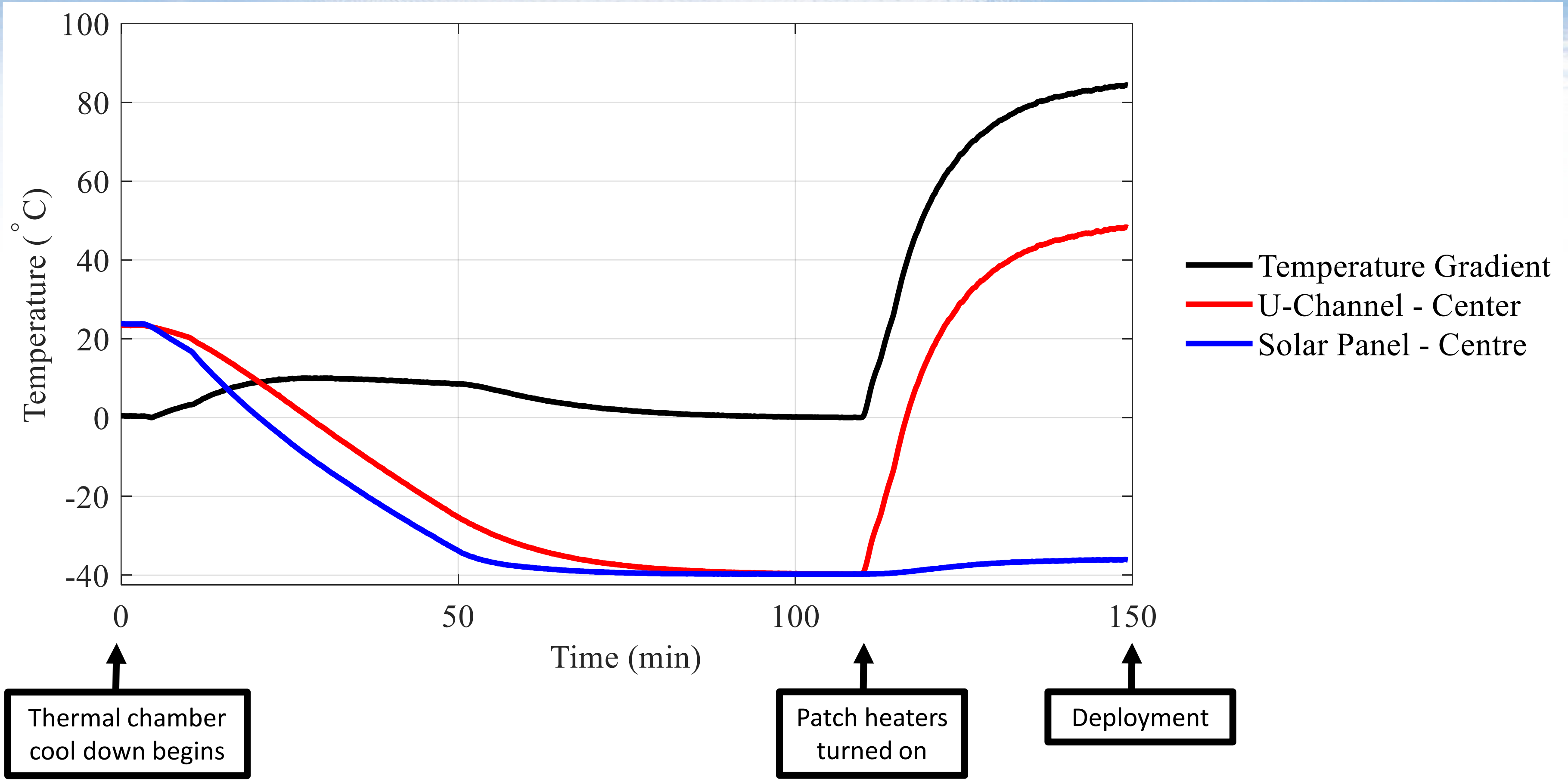

Thermal Chamber Deployment Test

Conclusion

- Supported hypothesis that differential thermal expansion was responsible for the partial deployment in TVAC
- To address thermal expansion issue, new hinge design sized with axial, radial clearances to give safety factor of 2 during expected orbital gradients

Addressing the issues

- Axial Interference: Increased clearance between swing & base leaves by removing material from base leaf through milling
- Radial Interference: Increasing clearance between shoulder bolt and sleeve bearing by increasing diameter of sleeve bearing using reamer
- Assembly alignment: Reduced misalignment by increasing precision of assembly through deployable panel assembly procedure, alignment GSE and process

Post-Vibe Test Partial Deployment

- Post-vibration deployment test resulted in partial deployment of one solar panel

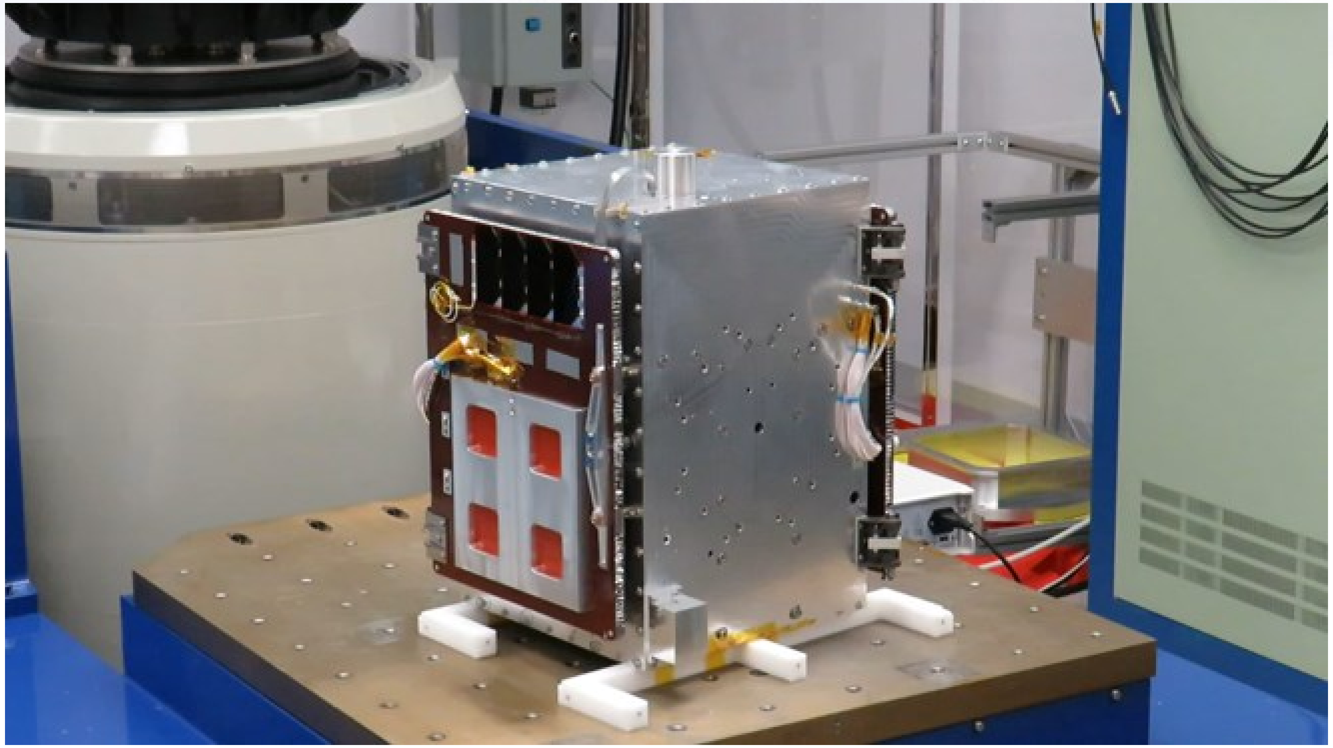

https://youtu.be/xim-nxDLiM0

Post-Vibe Test Partial Deployment

- Post-vibration test inspection revealed cracked cup interface
- Crack was caused by fatigue at sharp edge of cup
- Broken cup cannot constrain in-plane motion allowing slippage between swing leaf and solar panel Kapton interface
- Slippage exacerbated by the low friction coefficient of Kapton

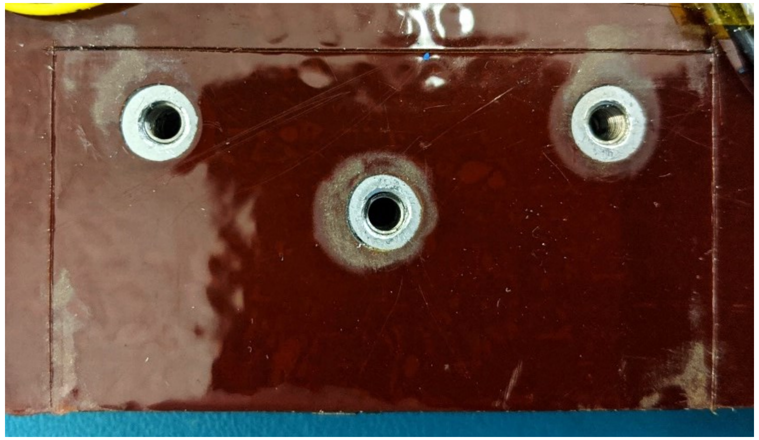

Post-Vibe Test Partial Deployment

Solutions:

- Mech team redesigned cup mounting features to reduce fatigue stress
- Increased friction coefficient in swing leaf to solar panel interface by replacing Kapton with stainless steel shim insert

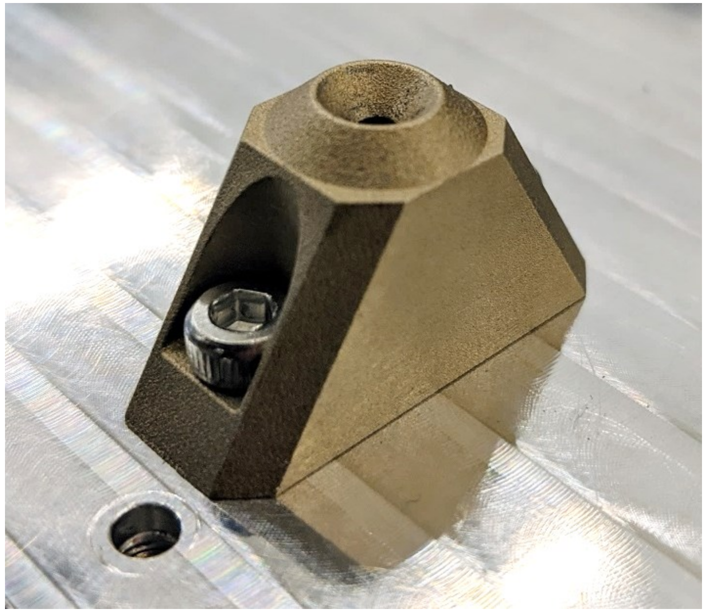

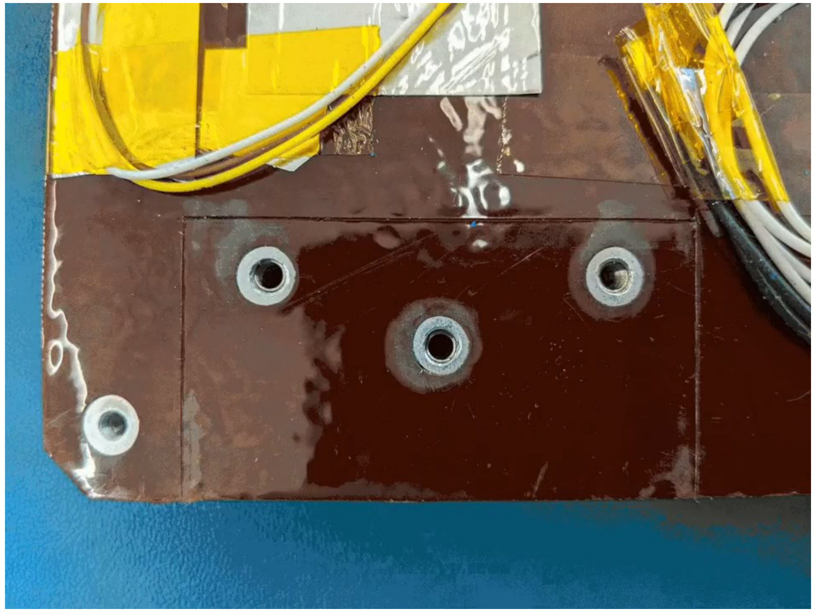

On-Orbit Operation

Commissioning

- Commissioning is the process of bringing a spacecraft into use
- All subsystems are checked out and components calibrated as needed

Deployment

https://youtu.be/E7Cf1-01W6A

https://youtu.be/uZrqXvg4J4E

https://youtu.be/UFI6uilof3c

GNC Subsystem Commissioning

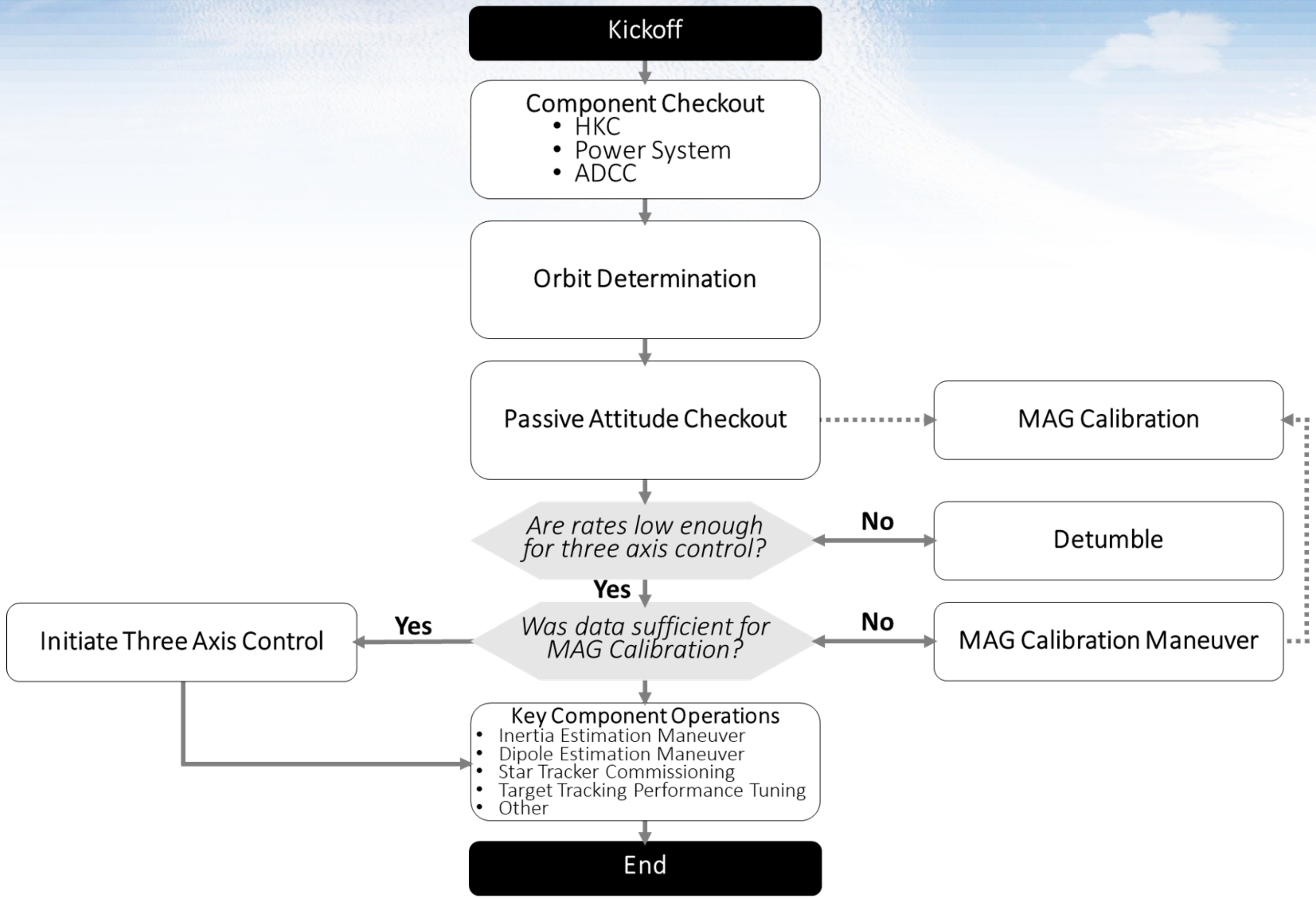

UTIAS SFL

Magnetometer Calibration

- Ground calibration prior to spacecraft integration is limited:
  - by accuracy of reference magnetometer used
  - fails to account for hard & soft iron bias introduced by spacecraft environment
- Magnetometer recalibrated in space to improve pointing accuracy

$$\underset{\mathbf{x}}{\text{minimize}} \quad \left|\left|\vec{\mathbf{B}}_{\mathrm{r},\,k}\right| - \left|\vec{\mathbf{B}}_{k}\left(\mathbf{x}\right)\right|\right|$$

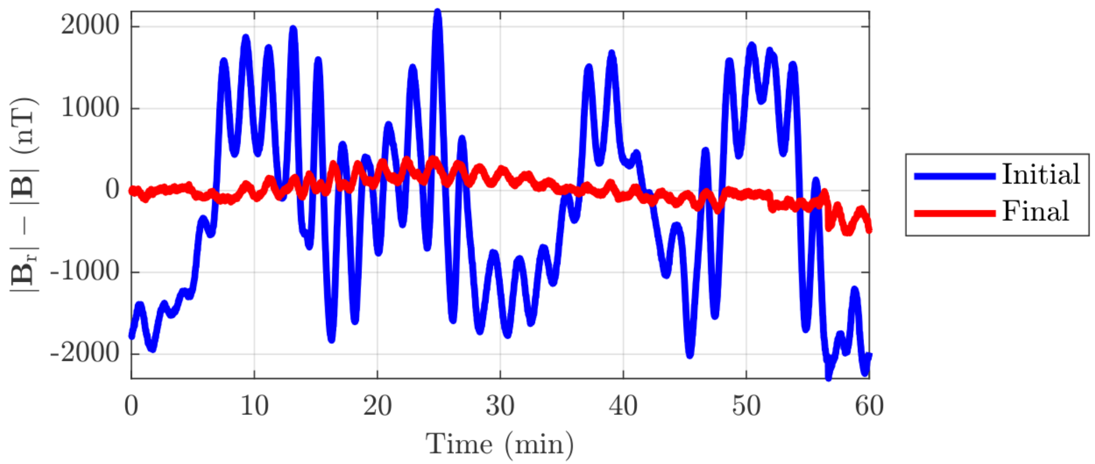

Magnetometer on-orbit measurement residuals, before and after on-orbit calibration

Residual Magnetic Dipole Estimation

- Spacecraft residual magnetic dipole m_r used in prediction step of attitude EKF
- **Maneuver:** Inertial attitude, momentum management disabled
- Can assume reaction wheel angular momentum change in body frame $\dot{h}_w$ due solely to disturbance torques τ_d
- Magnetic disturbance is largest, $\tau_r = m_r^{\times} B$
- Arrange into $\boldsymbol{Ax} = \boldsymbol{b}$ form and estimate m_r through least-squares approach

$$\dot{\mathbf{h}}_\mathrm{w} = \boldsymbol{\tau}_\mathrm{d} \rightarrow \dot{\mathbf{h}}_\mathrm{w} = \mathbf{m}_\mathrm{r}^{\times}\mathbf{B} + \boldsymbol{\tau}'_\mathrm{d}$$

$$\underbrace{-\mathbf{B}^{\times}}_{\mathbf{A}}\underbrace{\mathbf{m}_\mathrm{r}}_{\mathbf{x}} = \underbrace{\dot{\mathbf{h}}_\mathrm{w} - \boldsymbol{\tau}'_\mathrm{d}}_{\mathbf{b}}$$

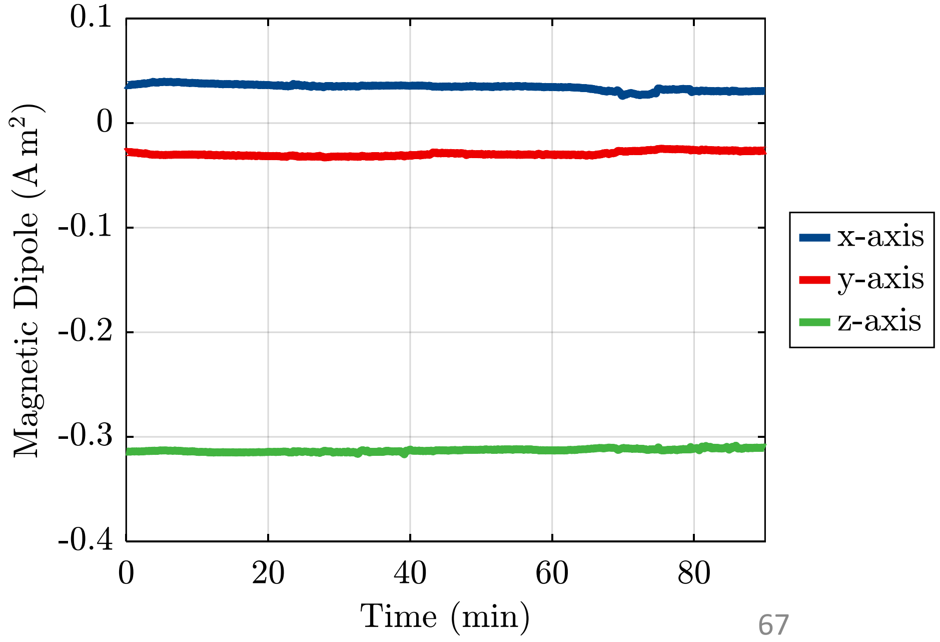

Inertia Estimation

- Used in prediction step of attitude EKF & feedforward terms of pointing controller
- CAD model is main source of estimate
- Inertia can change due to depletion of propellant
- **Inertia estimation maneuver:** Inertial attitude, momentum management disabled, reaction wheels then follow a speed profile
- Given short maneuver length, assuming system's angular momentum is conserved:

$$\mathbf{I}\dot{\boldsymbol{\omega}} + \boldsymbol{\omega}^{\times}\mathbf{I}\boldsymbol{\omega} = -\dot{\mathbf{h}}_{\mathrm{w}} - \boldsymbol{\omega}^{\times}\mathbf{h}_{\mathrm{w}}$$

- Inertia vector introduced for compact representation of inertia matrix:

$$\mathbf{I}_{\mathrm{v}} = \begin{bmatrix} I_{11} & I_{22} & I_{33} & I_{12} & I_{13} & I_{23} \end{bmatrix}^T \qquad \mathbf{I}\boldsymbol{\omega} = \boldsymbol{\Lambda}(\boldsymbol{\omega})\mathbf{I}_{\mathrm{v}}$$

- Arrange equation into $\boldsymbol{Ax} = \boldsymbol{b}$ form and estimate I_v through least-squares approach

$$\underbrace{\left(\boldsymbol{\Lambda}\left(\dot{\boldsymbol{\omega}}\right) + \boldsymbol{\omega}^{\times}\boldsymbol{\Lambda}\left(\boldsymbol{\omega}\right)\right)}_{\mathbf{A}} \underbrace{\mathbf{I}_{\mathrm{v}}}_{\mathbf{x}} = \underbrace{-\dot{\mathbf{h}}_{\mathrm{w}} - \boldsymbol{\omega}^{\times}\mathbf{h}_{\mathrm{w}}}_{\mathbf{b}}$$

Inertia Estimation

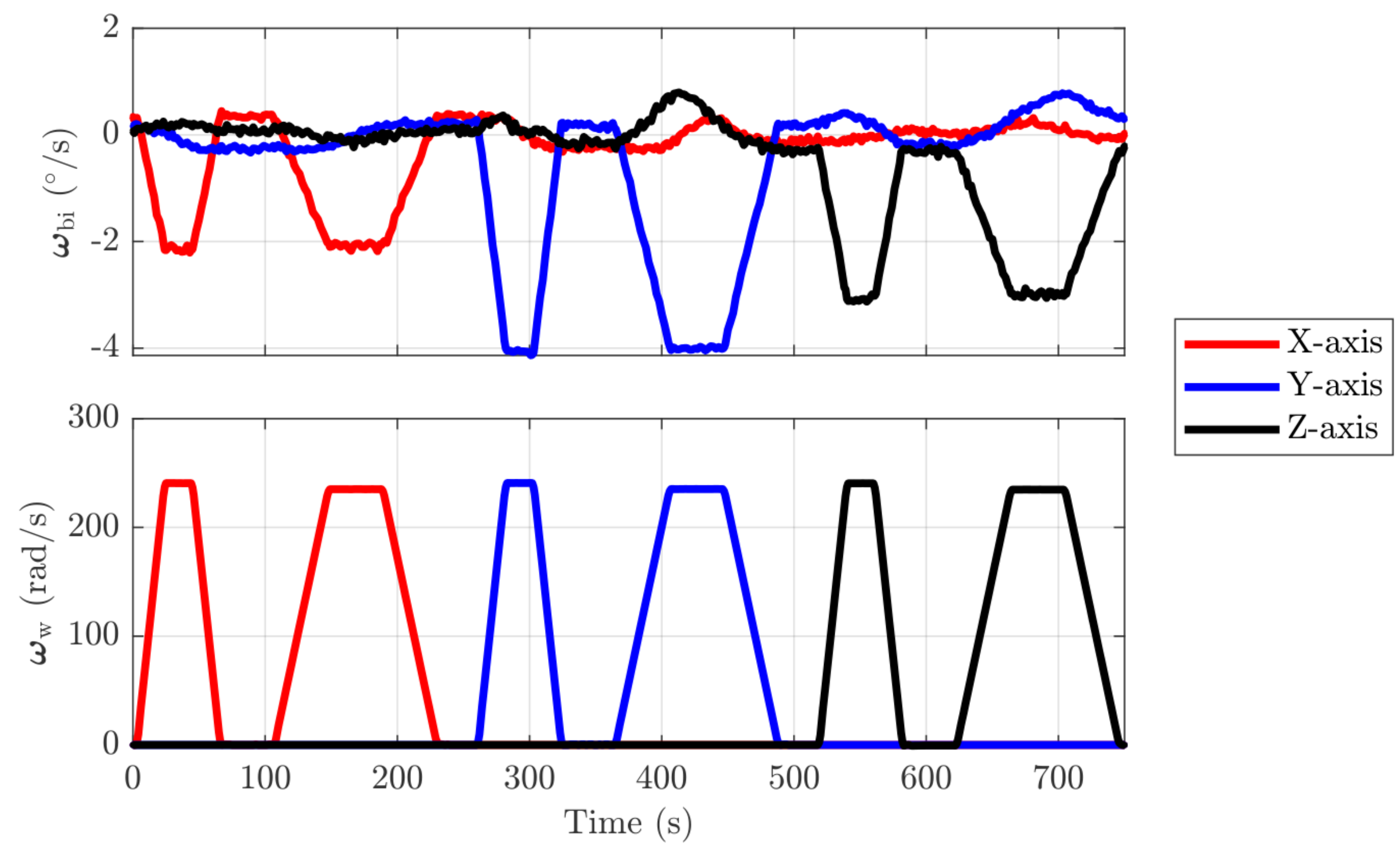

Reaction wheel and spacecraft angular velocity during inertia estimation maneuver

Reaction Wheel Momentum Setpoint

- Wheels' momentum varies due to attitude, orbit trajectory & environmental disturbance torque rejection
- Magnetorquer desaturates wheels through momentum management controller
- Controller can regulate to momentum setpoint in body or inertial frame:
  - **Body frame setpoint:** constant wheel speed but higher controller use, leads to worse attitude estimation and control errors, given MTQ dipole model accuracy limitations
  - **Inertial frame setpoint:** Well-chosen setpoint can take into account attitude, orbit trajectories during nominal operations, leading to lower controller use
- Reaction wheel speed resulting from the momentum setpoint should not be:
  - **Too low:** poor speed control, poor spacecraft pointing performance
  - **Too high:** decreased torque authority, accelerated wheel degradation

Reaction Wheel Momentum Setpoint

- Inertial momentum setpoint $h_{w,d,i}$ that will avoid undesirable wheel speeds and take into account nominal attitude, orbit trajectory, found by minimizing cost function within ROSA:

$$\underset{\mathbf{h}_{\mathrm{w,\,d,\,i}}}{\text{minimize}} \quad \sum_{k=1}^{m}\left(\prod_{j=1}^{n}\mathcal{C}(\omega_{\mathrm{w},\,j,\,k})\right)$$

$$\mathcal{C}\left(\omega_{\mathrm{w}}\right)=\begin{cases}-m|\omega_{\mathrm{w}}|+b_{\mathrm{l}} & \text{if} \qquad |\omega_{\mathrm{w}}|\leq\omega_{\mathrm{l}}\\ \mathrm{c_m} & \text{if } \omega_{\mathrm{l}}<|\omega_{\mathrm{w}}|\leq\omega_{\mathrm{h}}\\ m|\omega_{\mathrm{w}}|+b_{\mathrm{h}} & \text{if} \qquad |\omega_{\mathrm{w}}|>\omega_{\mathrm{h}}\end{cases}$$

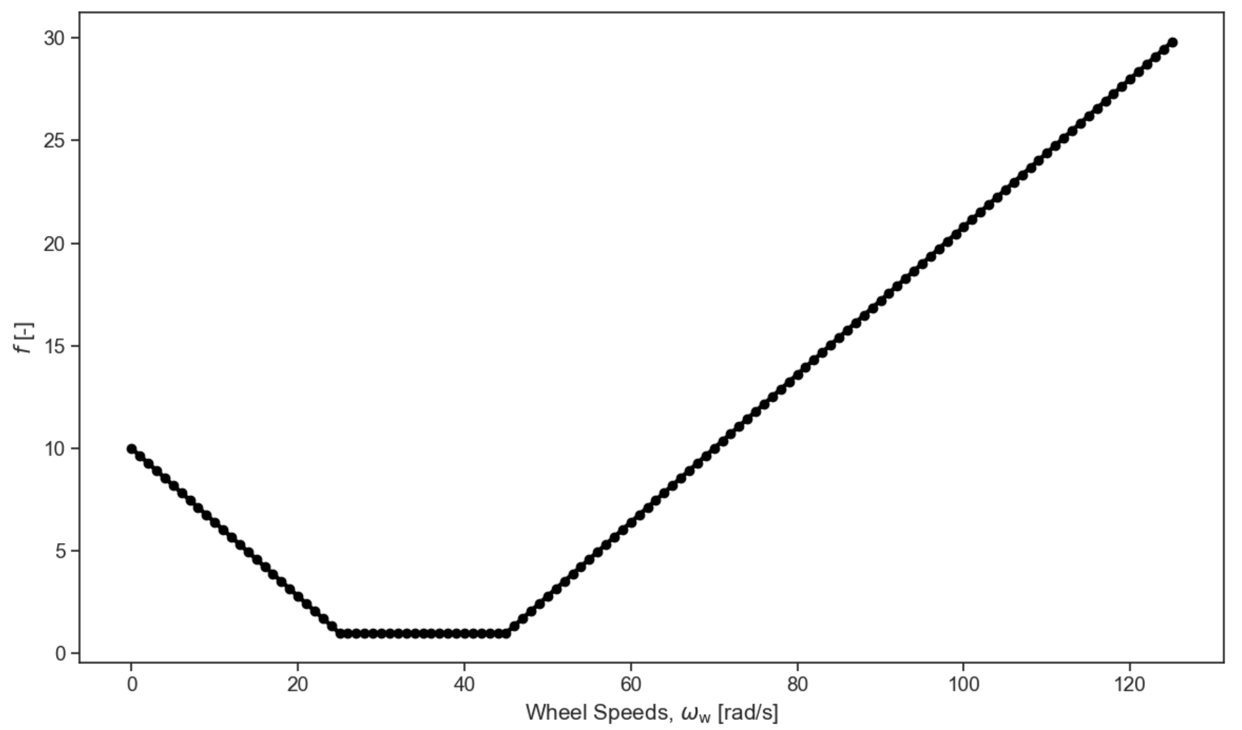

Reaction Wheel Momentum Setpoint

- Inertial momentum setpoint $h_{w,d,i}$ that will avoid undesirable wheel speeds and take into account nominal attitude, orbit trajectory, found by minimizing cost function within ROSA:

$$\underset{\mathbf{h}_{\mathrm{w,\,d,\,i}}}{\text{minimize}} \quad \sum_{k=1}^{m} \left(\prod_{j=1}^{n} \mathcal{C}(\omega_{\mathrm{w},\,j,\,k}) \right)$$

$$\mathcal{C}\left(\omega_{\mathrm{w}}\right) = \begin{cases} -m|\omega_{\mathrm{w}}| + b_{\mathrm{l}} & \text{if} \qquad |\omega_{\mathrm{w}}| \leq \omega_{\mathrm{l}} \\ \mathrm{c_m} & \text{if } \omega_{\mathrm{l}} < |\omega_{\mathrm{w}}| \leq \omega_{\mathrm{h}} \\ m|\omega_{\mathrm{w}}| + b_{\mathrm{h}} & \text{if} \qquad |\omega_{\mathrm{w}}| > \omega_{\mathrm{h}} \end{cases}$$

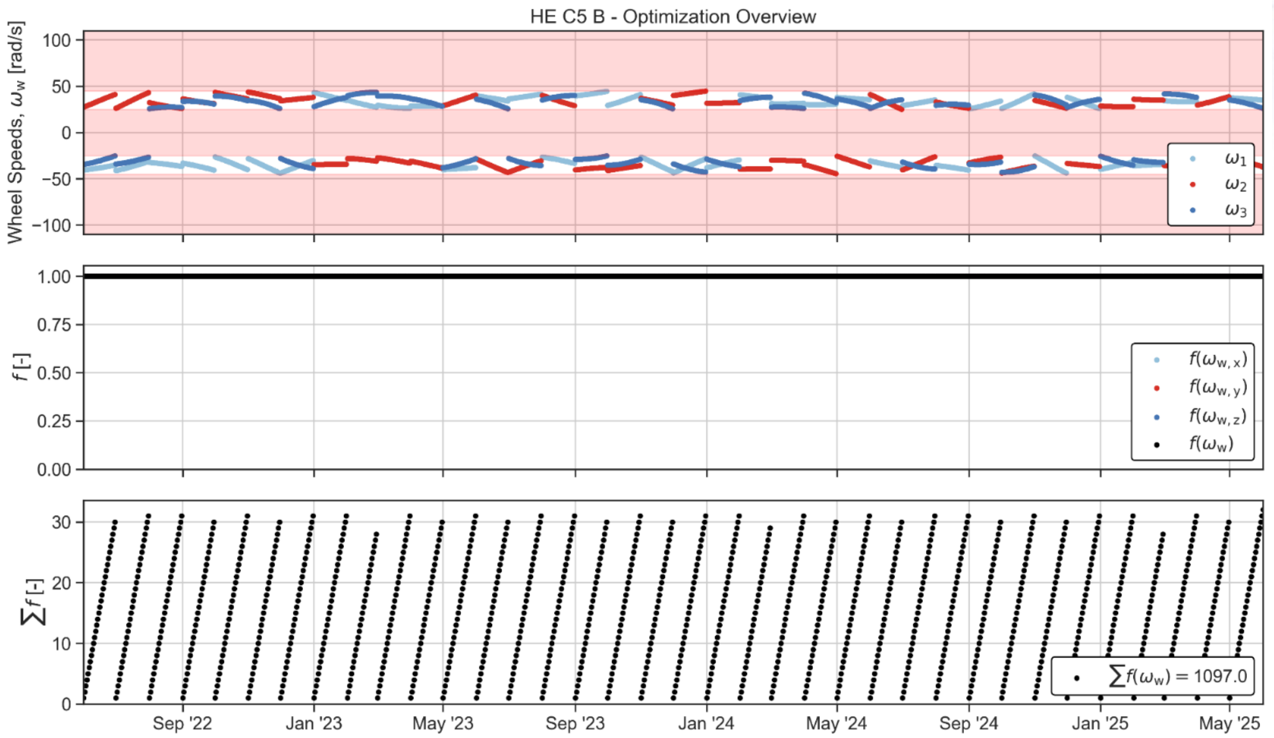

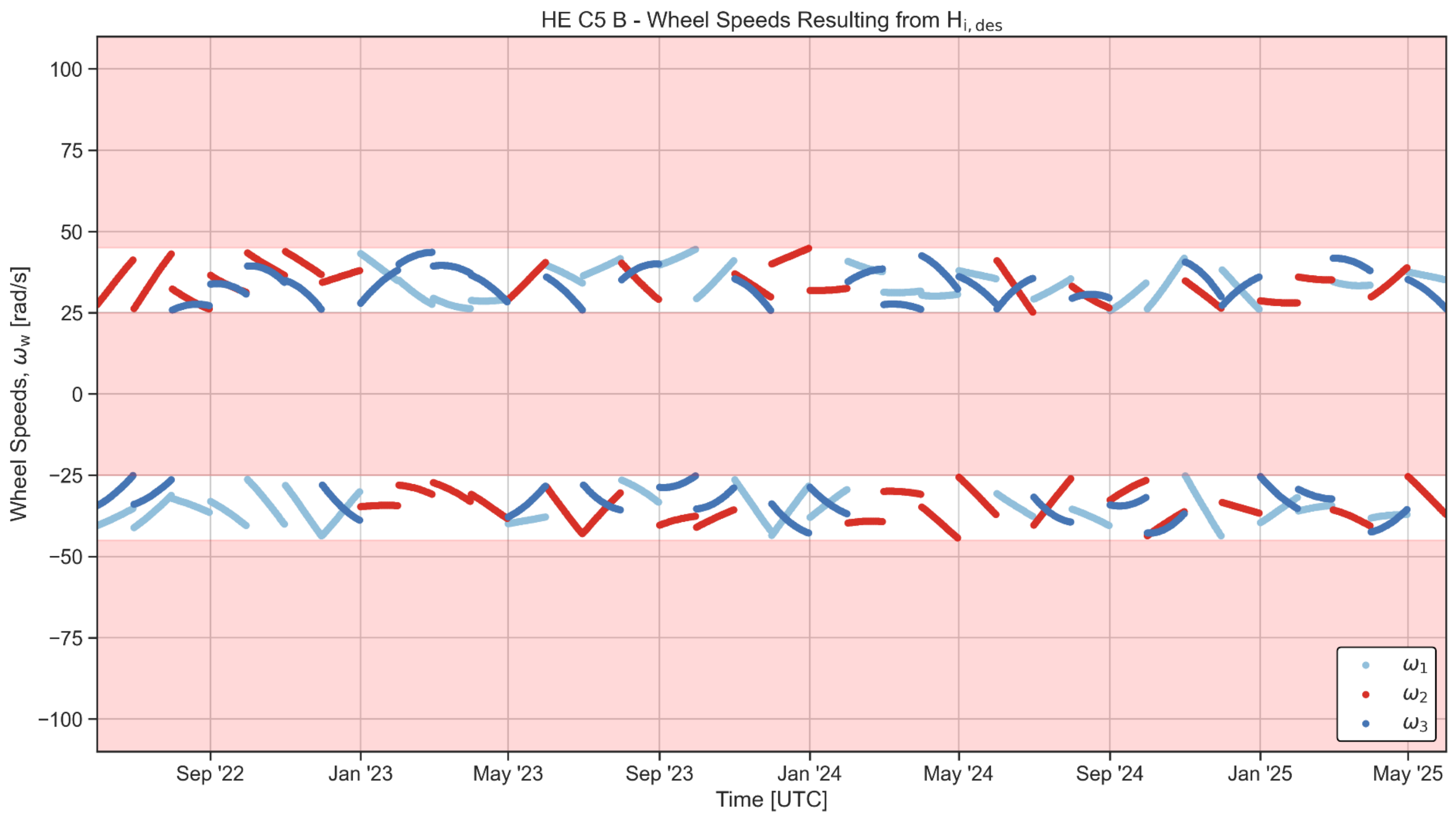

Reaction wheel speeds resulting from the numerical optimization methodology used to determine the inertial momentum setpoint at one-month intervals

Conclusion

- Covered the development of multiple spacecraft subsystems including the GNC, propulsion and deployable solar panel subsystems
- Testing process for spacecraft hardware presented and used in acceptance of GNC hardware for several spacecraft
- Qualification and acceptance of deployable solar panel subsystem were completed for several spacecraft
- Work covered was done with the hope of continuing to support the positive impact that satellites provide every day

Thank you for your time

Questions?